Geochemistry Geophysics Geosystems G3

Article
Volume 14, Number 10
4 October 2013
doi: 10.1002/ggge.20267
ISSN: 1525-2027

Published by AGU and the Geochemical Society

Constraints on past plate and mantle motion from new ages for the Hawaiian-Emperor Seamount Chain

John M. O'Connor
Alfred Wegener Institute for Polar and Marine Research, Bremerhaven, Germany

GeoZentrum Nordbayern, University Erlangen-Nuremberg, Erlangen, Germany

Deep Earth and Planetary Sciences, VU University Amsterdam, De Boelelaan 1085, 1081 HVAmsterdam, Netherlands (j.m.oconnor@vu.nl)

Bernhard Steinberger
Helmholtz Centre Potsdam—GFZ German Research Centre for Geosciences, Potsdam, Germany

The Centre for Earth Evolution and Dynamics, University of Oslo, Oslo, Norway

Marcel Regelous
GeoZentrum Nordbayern, University Erlangen-Nuremberg, Erlangen, Germany

Anthony A. P. Koppers
CEOAS, Oregon State University, Corvallis, Oregon, USA

Jan R. Wijbrans
Deep Earth and Planetary Sciences, VU University Amsterdam, Amsterdam, Netherlands

Karsten M. Haase
GeoZentrum Nordbayern, University Erlangen-Nuremberg, Erlangen, Germany

Peter Stoffers
Institute for Geosciences, Christian-Albrechts-University, Kiel, Germany

Wilfried Jokat
Alfred Wegener Institute for Polar and Marine Research, Bremerhaven, Germany

Dieter Garbe-Schönberg
Institute for Geosciences, Christian-Albrechts-University, Kiel, Germany

[1] Estimates of the relative motion between the Hawaiian and Louisville hot spots have consequences for understanding the role and character of deep Pacific-mantle return flow. The relative motion between these primary hot spots can be inferred by comparing the age records for their seamount trails. We report $^{40}Ar/^{39}Ar$ ages for 18 lavas from 10 seamounts along the Hawaiian-Emperor Seamount Chain (HESC), showing that volcanism started in the sharp portion of the Hawaiian-Emperor Bend (HEB) at $\geq$47.5 Ma and continued for $\geq$5 Myr. The slope of the along-track distance from the currently active Hawaiian hot spot plotted versus age is constant (57 $\pm$ 2 km/Myr) between $\sim$57 and 25 Ma in the central $\sim$1900 km of

the seamount chain, including the HEB. This model predicts an age for the oldest Emperor Seamounts that matches published ages, implying that a linear age-distance relationship might extend back to at least 82 Ma. In contrast, Hawaiian age progression was much faster since at least ~15 Ma and possibly as early as ~27 Ma. Linear age-distance relations for the Hawaii-Emperor and Louisville seamount chains predict ~300 km overall hot spot relative motion between 80 and 47.5 Ma, in broad agreement with numerical models of plumes in a convecting mantle, and paleomagnetic data. We show that a change in hot spot relative motion may also have occurred between ~55 Ma and ~50 Ma. We interpret this change in hot spot motion as evidence that the HEB reflects a combination of hot spot and plate motion changes driven by the same plate/mantle reorganization.

Components: 14,074 words, 9 figures, 3 tables.

Keywords: hot spots; plumes; seamounts; mantle geodynamics; plate motion; Hawaiian-Emperor seamounts.

Index Terms: 3037 Oceanic hotspots and intraplate volcanism: Marine Geology and Geophysics; 8137 Hotspots, large igneous provinces, and flood basalt volcanism: Tectonophysics; 8121 Dynamics: convection currents, and mantle plumes: Tectonophysics; 1115 Radioisotope geochronology: Geochronology.

Received 14 May 2013; **Revised** 9 August 2013; **Accepted** 4 September 2013; **Published** 4 October 2013.

O'Connor, J. M., B. Steinberger, M. Regelous, A. A. P. Koppers, J. R. Wijbrans, K. M. Haase, P. Stoffers, W. Jokat, and D. Garbe-Schönberg (2013), Constraints on past plate and mantle motion from new ages for the Hawaiian-Emperor Seamount Chain, *Geochem. Geophys. Geosyst.*, *14*, 4564–4584, doi:10.1002/ggge.20267.

1. Introduction

[2] Age-progressive volcanism in the Hawaiian-Emperor seamount chain, and the fact that this is largely unaffected by the occurrence of the classic "elbow" in the middle, the so-called Hawaiian-Emperor Bend (HEB), are key observations underpinning the hypothesis that seamount chains form as tectonic plates drift relative to fixed or slowly moving hot spots [*Wilson*, 1963]. Hot spots are generally held to be maintained by deep-seated mantle plumes or upwellings [*Morgan*, 1971] rising from a mantle boundary layer (either the core-mantle boundary, or the phase transition at 660 km depth). An alternative to this "bottom-up" model is a "top-down" plate-driven process in which rifting of the lithosphere triggers shallow mantle melting [*Anderson*, 2000], although, as discussed by *Tarduno et al*. [2009], these alternative mechanisms (e.g., propagating cracks) may be insufficient [*Sleep*, 2007] to explain the large volume flux and longevity of the Hawaiian hot spot and the geometry of its track. The seismic data of *Wolfe et al*. [2009] show a zone of low velocities in the mantle beneath Hawaii that is compatible with an upwelling plume. These images indicate that the plume conduit is tilted, coming up from the southeast, consistent with dynamic plume models [*Steinberger*, 2000]. Such good agreement between seismic image and model prediction gives additional support to a deep plume origin, but it might further be possible to test between "bottom-up" and "top-down" end-member models using improved age records for long-lived Pacific hot spot chains.

[3] Recent studies using the age records and geometries of Pacific hot spot trails conclude that they cannot fit the predictions of the fixed hot spot hypothesis without invoking at least some hot spot drift [*Koppers et al*., 2001, 2004; *Wessel and Kroenke*, 2008, *Koppers et al*., 2011]. Others confine this drift only to very specific periods when, for example, the older Emperor and Louisville seamounts were forming [*Wessel et al*., 2006; *Andrews et al*.; 2006; *Wessel and Kroenke*, 2008, 2009, *Koppers et al*., 2011]. In addition, global plate reconstructions are unable to predict the HEB [*Molnar and Stock*, 1987; *Cande et al*., 1995; *Raymond et al*., 2000] and pronounced shifts in paleolatitude over time imply a ~40–50 km/Myr southward motion of the Hawaiian hot spot during formation of the Emperor seamount chain, which ceased at ~47 Ma in the HEB [*Tarduno et al*., 2003; *Tarduno*, 2007; *Tarduno et al*.; 2009]. This age-progressive shift in paleolatitude is consistent with south-south-eastward hot spot motion predicted by the modeling of the temporal evolution of a plume conduit embedded in mantle flow back in time [*Steinberger*, 2000; *Steinberger and O'Connell*, 2000; *Steinberger et al*., 2004;

Doubrovine et al., 2012]. However, the modeled hot spot motion during the past 100 Myr can vary from a few 100 km to more than 1000 km, largely depending on the estimated hot spot (plume) initiation age. Since the starting age of the Hawaiian hot spot is unknown (the oldest part of the Emperor chain has been subducted), there is enough flexibility in choosing an initiation age such that the measured age-progressive paleolatitude is approximately matched in these numerical models [*Tarduno et al*., 2003]. These models, though, are generally interpreted as predicting a more gradual slowdown in hot spot motion, whereas paleolatitudes indicate a rather abrupt stop at the time of the bend. *Tarduno et al*. [2009] propose that the Hawaiian plume may have been captured by a spreading centre, followed by its release after the spreading ridge migrated away from the hot spot during formation of the Emperor Seamounts.

[4] $^{40}Ar/^{39}Ar$ age dating and palaeomagnetic inclination data from four Louisville seamounts indicate that this hot spot has remained within 3–5° of its present-day latitude of about 51°S between 70 and 50 million years ago, suggesting that the Louisville and Hawaiian hot spots are moving independently, and not as the result of a large-scale Pacific mantle "wind" [*Koppers et al*., 2012]. In view of the significance of the Hawaiian-Emperor Seamount Chain and the HEB for understanding plate motion and mantle geodynamics [e.g., *Tarduno et al*., 2009], it is important that current concepts and models are tested on the basis of an unambiguous, directly measured age record for the Hawaiian-Emperor chain, the HEB, and another long-lived copolar seamount chain, such as the Louisville Seamount trail.

[5] This manuscript reports highly reproducible mineral $^{40}Ar/^{39}Ar$ ages from dredge samples from the first new sampling in decades of the Hawaiian-Emperor Bend and western (older) ~1200 km of the Hawaiian seamount chain. We will arrive at a new and more arcuate direct age estimate for the most acuate part of the HEB and we will discuss implications of our new $^{40}Ar/^{39}Ar$ ages for estimates of the rate of propagation of magmatism along the Hawaiian seamount chain. The data are compared to new ages for Louisville Seamount Chain lavas [*Koppers et al*., 2004, 2011, 2012] in order to determine the relative motion between the Louisville and Hawaiian hot spots since the Cretaceous, and thus place new constraints on past changes in Pacific plate motion and mantle flow.

2. Samples and $^{40}Ar/^{39}Ar$ Data

2.1. Sampling

[6] During the SO141 "HULA" Expedition we used the RV *Sonne* to dredge sample and swath map the Hawaiian-Emperor Bend and northern half of the Hawaiian Seamount Chain (Figure 1) [*Ackermand et al*., 1999]. Sampling began at Yuryaku and Daikakuji seamounts, located in the arcuate part of the Hawaiian-Emperor Bend (Figure 1). After sampling the HEB, recently redated to 46.8 ± 0.1 Ma [*Sharp and Clague*, 2006], we continued sampling eastward as far as Midway Atoll, previously dated to 28.7 ± 0.6 Ma using subaerial drill hole samples [*Dalrymple et al*., 1977; *Clague and Dalrymple*, 1989]. Sample locations are in Table 1 and descriptions and geochemical compositions are available in supporting information.

2.2. Sample Preparation

[7] Samples were crushed and sieved into 250–125 μm, 150–74 μm, or 74–48 μm size fractions. Plagioclase was separated from the 250 to 125 μm fraction using a paramagnetic separator and from the 150–74 μm and 74–48 μm fractions by a combination of heavy liquid and paramagnetic methods. The samples were cleaned with combinations of HF, HCl, and HNO_3 (see Table 2) and finally washed in distilled H_2O in an ultrasonic bath.

2.3. $^{40}Ar/^{39}Ar$ Methodology

[8] Samples were irradiated in the cadmium-shielded CLICIT facility in the TRIGA reactor at Oregon State University and incrementally heated at the Laserprobe dating facility at the VU University Amsterdam. Data acquisition and reduction, corrections for mass discrimination and age calculation have been described in detail previously [*Koppers et al*., 2000; *Koppers*, 2002; *O'Connor et al*., 2004; *Kuiper et al*., 2008]. Due to seawater alteration (see sample descriptions and geochemistry in supporting information), we report ages for mineral separates that were reproducible at the 2σ uncertainty level between replicated sets of analyses (Table 2). Ages have been calculated using the Freeware program ArArCALC [*Koppers*, 2002] and the decay constant of *Steiger and Jaeger* [1977] and we have made all the ArArCALC data files available in supporting information. Note that a detailed description of ArArCALC tables and plots is available in supporting information for *Koppers et al*. [2012]. The new Hawaiian seamount ages have been measured relative to the

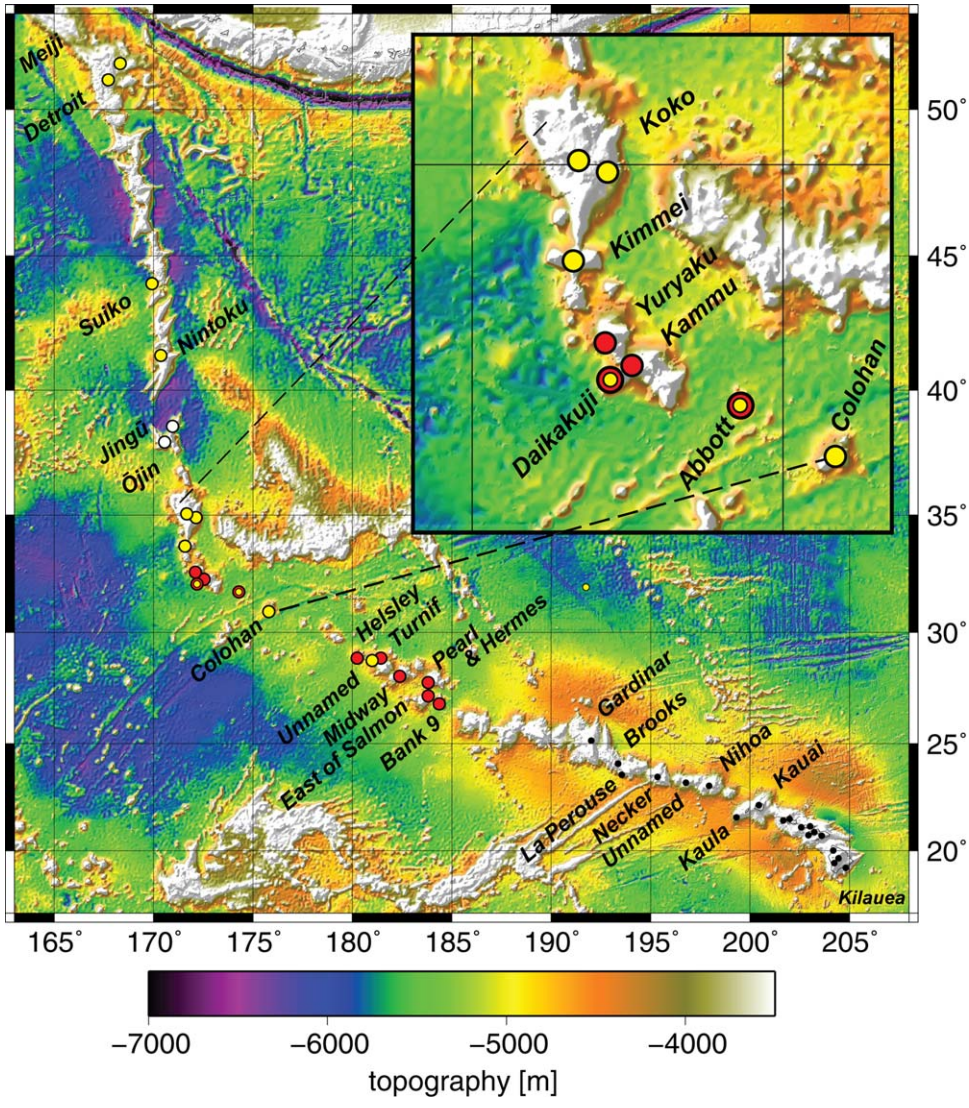

Figure 1. Topography map [*Smith and Sandwell*, 1997] of the Hawaiian-Emperor Seamount Chain created with GMT software [*Wessel and Smith*, 1991]. Red symbols show locations of the samples used in this study, yellow symbols are sample locations for post-1995 cited ages [*Sharp and Clague*, 2006; *Duncan and Keller*, 2004, *Keller et al*., 1995] and large white are for pre-1995 Ōjin and Jingū seamount ages [*Dalrymple et al*., 1980; *Dalrymple and Garcia*, 1980]. Small black symbols are for locations of dated samples in the young Hawaiian islands and seamounts (data sources in *Clague and Dalrymple* [1989] and isotopic age recalibration database available as supporting information).

TCR-2 sanidine standard with an assigned age of 28.34 ± 0.28 Ma (2σ) [*Renne et al*., 1998] as the flux monitor.

[9] All data from the literature quoted in this paper have been recalibrated to 28.34 ± 0.28 Ma age of TCR-2 standard [*Renne et al*., 1998] using the ArArCALIBRATIONS v2.0 Freeware Tool (provided by A.A.P. Koppers as Freeware on http://earthref.org/ararcalc.htm) (see supporting information). This allows direct comparisons between $^{40}Ar/^{39}Ar$ ages from studies on both the Hawaiian-Emperor and Louisville seamount trails. As we are combining data from numerous data sources, collected by different laboratories over many decades, and using different age standards or different assigned age values, it is critical to carry out these recalibrations, as the recalibrated ages can be ~1–2 Myr older than the reported ages. As an example, the 81.2 ± 1.3 Ma age for the Detroit Seamount reported by *Keller et al*. [1995] becomes 82.3 ± 1.3 Ma using the *Renne et al*. [1998] TCR standard with an assigned age of 28.34 Ma. Another example, the 55.4 ± 0.9 Ma age for Jingū

Table 1. Sample Locations in the Hawaiian-Emperor Seamount Chain

		Location	Depth (mbsf)
		On Bottom[a]	On Bottom[a]
Sample	Seamount	Off Bottom[b]	Off Bottom[b]
SO141-5DR	Yuryaku	32° 33.61 N 172° 11.31 E	3022
		32° 34.55 N 172° 12.03 E	2251
SO141-6DR-3	Daikakuji	32° 04.48 N 172° 10.32 E	3780
		32° 05.33 N 172° 12.82 E	2170
SO141-9DR-1	North Kammu	32° 16.86 N 172° 37.11 E	2876
		32° 16.76 N 172° 37.37 E	2802
SO141-12DR-1	Abbott	31° 48.65 N 174° 15.05 E	3593
		31° 48.66 N 174° 15.75 E	3180
SO141-23DR-3	Helsley	28° 56.33 N 179° 42.27 W	3015
		28° 55.81 N 179° 40.81 W	2297
SO141-25DR-1	Turnif	28° 52.40 N 178° 29.71 W	2533
		28° 52.73 N 178° 30.34 W	2093
SO141-29DR-1	Midway	28° 01.47 N 177° 31.21 W	2938
		28° 05.63 N 177° 30.13 W	1589
SO141-34DR-1	Pearl and Hermes	27° 45.79 N 176° 09.14 W	2610
		27° 46.50 N 176° 07.54 W	1918
SO141-37DR-1	Bank 9	26° 52.29 N 175° 33.82 W	2979
		26° 52.31 N 175° 35.09 W	2135
SO141-38DR-1	East of Salmon	27° 12.72 N 176° 08.50 W	2639
		27° 12.35 N 176° 09.04 W	2280

[a]Location/depth of dredge on seamount at the start of sampling.
[b]Location/depth of dredge on seamount at the end of sampling.

Seamount and 55.2 ± 0.7 Ma age for Ōjin Seamount become 57.3 ± 0.9 Ma and 57.1 ± 0.7 Ma, respectively, using the *Lanphere and Dalrymple* [2000] 62ALe-I or SB-3 standard with an assigned age of 160.2 Ma. All ages in this paper are reported as 2σ uncertainties.

2.4. Data Quality

[10] The new $^{40}Ar/^{39}Ar$ ages reported here (Table 2) meet the following acceptability criteria and thresholds:

[11] 1. Experiments were carried out on plagioclase phenocryst and microphenocryst phases, because they are more resistant to hydrothermal and seawater alteration processes compared to their groundmass.

[12] 2. $^{40}Ar/^{39}Ar$ ages have been successfully replicated at least once and in many instances twice.

[13] 3. Plateaus contain at least 70% of the total released ^{39}Ar; however, most analyses reported here have significantly more: 70–79% (3 analyses), 80–89% (11 analyses), 90–99% (11 analyses), and 100% (15 analyses).

[14] 4. Plateaus have a minimum of seven incremental heating steps, however many have significantly more: 8 (4 analyses), 9 (9 analyses), 10 (4 analyses) 11 (11 analyses), 12 (4 analyses), 13 (4 analyses), 14 (1 analysis).

[15] 5. Isochrons are concordant with plateau ages within analytical uncertainty with a single exception (9–16), the age of which has however been replicated by two different samples from the same dredge haul (9–1 and 9–13).

[16] 6. Support for the reliability of our new ages is shown by the agreement between our new 41.4 ± 0.7 Ma age and an existing age of 41.6 ± 1.3 Ma for Abbott Seamount [*Sharp and Clague*, 2006], and between our new 27.5 ± 1.2 Ma age and a published 28.7 ± 0.6 Ma age for Midway Atoll [*Clague and Dalrymple*, 1989]. Our ~47.5 ± 0.5 Ma age for shield lavas from Daikakuji corresponds well with a 46.8 ± 0.1 Ma existing age for a shield basalt from Daikakuji [*Sharp and Clague*, 2006].

[17] 7. The accuracy of our new ages is also generally supported by the geochemistry of the dated samples (see detailed discussion in section 3.4.). Studies of young, subaerial Hawaiian volcanoes have shown that in most cases tholeiitic lavas that were erupted within 1 Myr are overlain by alkali lavas, which may be up to 2 Myr younger. These in turn are overlain by highly alkalic, silica-undersaturated lavas which can be as much as 6 Myr younger than the oldest tholeiitic lavas [e.g.,

Table 2. $^{40}Ar/^{39}Ar$ Analyses of SO141 Lavas from the Hawaiian-Emperor Seamount Chain

			Plateau Age					Total Fusion	Inverse Isochron Analysis				
Sample	Lab ID	Grainsize (μm)	Age (Ma)	%^{39}Ar	K/Ca	MSWD[a]	n[b]	Age (Ma)	Age (Ma)	$^{40}Ar/^{36}Ar$ Intercept	MSWD[a]	Angle[c]	Km[c]
Yuryaku Seamount													
5-6 (S)	04M0146	[1]74-48	31.6 ± 0.4	77	0.02	0.5	9	32.6 ± 0.5	30.6 ± 1.3	337 ± 52	0.1	32.18	3576
5-6 (S)	04M0106	[1]74-48	31.6 ± 0.7	80	0.02	0.2	7	31.6 ± 0.7	31.2 ± 1.1	308 ± 25	0.04		
5-6 (S)	06MY271	[1]74-48	31.7 ± 0.4	72	0.02	0.7	11	32.3 ± 0.4	31.0 ± 1.0	319 ± 29	0.4		
5-8 (S)	04M0147	[1]74-48	31.7 ± 0.4	79	0.02	0.4	9	32.7 ± 0.4	31.4 ± 0.9	304± 34	0.4	32.18	3576
5-8 (S)	04M0108	[1]74-48	31.9 ± 0.7	84	0.01	0.6	8	31.0 ± 0.8	31.5 ± 1.2	306 ± 28	0.6		
5-8 (S)	06MY270	[1]74-48	31.6 ± 0.5	81	0.02	1.0	13	32.5 ± 0.6	30.8 ± 1.0	317 ± 20	0.6		
5-10 (S)	04M0213	[2]150-74	43.2 ± 0.7	93	0.01	0.4	11	43.0 ± 0.7	43.1 ± 0.8	310 ± 42	0.4	32.18	3576
5-10 (S)	04M0126	[2]150-74	42.7 ± 1.4	100	0.01	0.2	11	42.6 ± 1.7	42.8 ± 1.5	288 ± 53	0.2		
5-10 (S)	06MY075	[2]150-74	43.1 ± 0.9	84	0.01	0.7	8	42.6 ± 0.8	43.3 ± 1.5	285 ± 74	0.8		
5-11 (S)	04M0163	[1]74-48	45.0 ± 0.4	94	0.03	0.8	12	44.8 ± 0.5	44.9 ± 1.1	298 ± 30	0.8	32.18	3576
5-11 (S)	04M0112	[1]74-48	44.9 ± 0.6	86	0.03	0.4	8	44.2 ± 0.6	45.2 ± 1.0	289 ± 21	0.4		
5-11 (S)	06MY275	[1]74-48	45.1 ± 0.4	100	0.03	0.1	14	45.1 ± 0.5	45.1 ± 0.6	295 ± 10	0.2		
5-20 (LS)	04M0165	[1]74-48	47.4 ± 0.5	88	0.01	0.1	10	46.9 ± 0.5	47.6 ± 2.2	289 ± 59	0.15	32.18	3576
5-20 (LS)	04M0115	[1]74-48	47.3 ± 0.9	85	0.01	0.02	7	45.9 ± 0.4	47.3 ± 4.9	295 ± 117	0.02		
5-20 (LS)	06MY292	[1]74-48	47.3 ± 0.6	81	0.01	0.1	11	46.6 ± 0.6	47.2 ± 3.4	299 ± 106	0.15		
Daikakuji Seamount													
6-3 (PS)	04M0225	[1]74-48	47.3 ± 1.1	96	0.01	0.1	11	47.2 ± 1.2	47.2 ± 5.1	297 ± 55	0.1	32.03	3559
6-6 (LS)	04M0230	[1]74-48	47.5 ± 0.5	100	0.01	0.1	12	47.5 ± 0.6	47.6 ± 1.0	294 ± 16	0.1	32.03	3559
6-7 (LS)	04MY377	[2]250-150	47.5 ± 0.9	92	0.01	0.1	9	47.8 ± 1.1	46.8 ± 2.8	380 ± 296	0.1	32.03	3559
6-7 (LS)	06MY181	[2]250-150	47.5 ± 0.9	100	0.01	0.4	12	47.6 ± 1.0	47.3 ± 1.0	300 ± 10	0.3		
6-7 (LS)	04M0215	[2]150-74	47.5 ± 0.7	100	0.01	0.2	10	47.5 ± 0.7	47.3 ± 0.8	307 ± 37	0.1		
6-7 (LS)	04M0226	[1]74-48	47.5 ± 0.5	98	0.02	0.6	11	47.6 ± 0.5	47.3 ± 0.7	302 ± 12	0.5		
6-7 (LS)	06MY276	[2]150-74	47.4 ± 1.1	99	0.01	0.03	11	49.0 ± 1.2	47.3 ± 3.6	297 ± 194	0.04		
Kammu Seamount													
9-1 (LS)	04M0132	[3]250-150	43.7 ± 0.6	100	0.02	0.2	9	43.9 ± 0.8	43.8 ± 0.8	295 ± 71	0.2	31.76	3529
9-1 (LS)	06MY293	[3]250-150	43.7 ± 0.5	100	0.02	0.1	10	43.8 ± 0.6	43.7 ± 0.8	297 ± 80	0.1		
9-13 (LS)	04M0133	[3]250-150	43.6 ± 0.5	100	0.02	0.5	10	43.5 ± 0.6	43.8 ± 0.6	258 ± 64	0.4	31.76	3529
9-16 (PS)	04M0134	[3]250-150	44.0 ± 0.7	98	0.01	0.4	9	40.3 ± 1.1	38.6 ± 4.2	381 ± 136	0.4	31.76	3529
Abbott Seamount													
12-1(S)	04M0216	[2]150-74	41.4 ± 0.7	88	0.01	0.1	9	40.6 ± 0.7	40.9 ± 1.8	320 ± 90	0.1	30.26	3362
12-1 (S)	06MY074	[2]150-74	41.4 ± 0.5	83	0.01	0.1	6	39.9 ± 0.5	41.3 ± 1.1	299 ± 20	0.1		
12-1 (S)	04M0127	[2]150-74	41.3 ± 0.9	92	0.01	0.7	8	40.3 ± 1.1	38.6 ± 4.2	381 ± 136	0.4		
Helsley Seamount													
23-3 (PS)	04M0242	[2]74-48	31.7 ± 1.0	99	0.01	0.1	11	31.9 ± 1.5	31.6 ± 1.1	299 ± 11	0.03	24.44	2716
23-3 (PS)	06MY289	[2]74-48	32.0 ± 1.0	100	0.01	0.1	13	32.1 ± 1.2	31.8 ± 2.1	302 ± 53	0.1		
Turnif Seamount													
25-1 (PS)	04M0244	[1]74-48	29.3 ± 0.6	92	0.001	0.4	11	32.2 ± 4.9	28.6 ± 1.2	305 ± 14	0.2	23.45	2606
25-1 (PS)	06MY076	[1]74-48	29.3 ± 0.7	100	0.001	0.8	9	31.5 ± 7.2	28.9 ± 1.6	300 ± 17	0.9		
Midway Atoll													
29-1 (S)	04M0246	[2]74-48	27.5 ± 1.2	100	0.01	0.1	12	28.7 ± 3.7	27.4 ± 1.2	298 ± 8	0.1	22.36	2485
29-1 (S)	06MY290	[2]74-48	27.6 ± 0.9	100	0.01	0.2	13	27.7 ± 1.0	27.2 ± 1.2	308 ± 22	0.1		
Pearl & Hermes Atoll													
34-1 (PS)	04M0247	[2]74-48	24.7 ± 0.3	97	0.02	0.6	11	24.7 ± 0.4	24.6 ± 0.4	301 ± 11	0.6	21.11	2346
34-1 (PS)	04M0089	[2]74-48	24.5 ± 0.8	100	0.02	0.3	11	23.9 ± 1.7	25.0 ± 2.4	274 ± 125	0.3		
34-1 (PS)	06MY077	[2]74-48	24.6 ± 0.5	100	0.02	0.8	9	24.6 ± 0.5	24.6 ± 0.8	297 ± 17	1.0		
Bank 9 Seamount													
37-1	04MY373	[2]74-48	82.0 ± 1.3	89	0.02	0.4	13	80.2 ± 1.7	81.5 ± 2.3	329 ± 186	0.3	20.36	2262
East of Salmon Seamount													
38-1[d]	00M0240	500-250	91.7 ± 0.6	94	0.6	0.1	10	93.4 ± 0.7	91.6 ± 0.8	300 ± 30	0.1	20.94	2327

Ages are calculated using TCR monitor age of 28.34 Ma [*Renne et al*., 1998].

$^{40}Ar/^{39}Ar$ ages were measured using the argon laser probe at the VU University Amsterdam.

Measured ages have been calculated using the Freeware software ArArCalc [*Koppers*, 2002].

$\lambda = 5.543 \times 10^{-10}$/yr.

Correction factors: $^{40}Ar/^{39}Ar$ (K) = 0.00086, $^{36}Ar/^{37}Ar$ (Ca) = 0.00026, and $^{39}Ar/^{37}Ar$ (Ca) = 0.00067.

[a]MSWD values for the age plateaus and inverse isochrons are calculated using N-1 and N-2 degrees of freedom, respectively.

[b]n is for the number of included heating steps.

[c]Distance along track of sampled volcanoes from the present hot spot at Kilauea (19.2°N, 155.05°W) with the H-E Bend at 32.546°N, 172.266°E.

[d]Rock chips, see sample preparation details in *O'Connor et al*. [2004].

S = shield stage; LS = late shield stage; PS = postshield stage.

[1]1N HNO_3 (60 min), [2]5% HF (1 min), 1N HNO_3 (60 min), [3]5 N HCl (60 min), HF 6-7% (5 MIN), and 1N HNO_3 (60 min).

Clague and Dalrymple, 1989]. On Pearl and Hermes Reef, Daikakuji and Kammu Seamounts, we obtained identical ages within error for different samples of transitional to alkalic lava, as expected. However, on Yuryaku Seamount we obtained an apparently wide spread of ages for five tholeiitic lava samples, which by analogy with young Hawaiian volcanoes, would be expected to have been erupted within a 1 Myr period.

3. Results

3.1. Linear Relation Between Age and Distance Since ~57 Ma

[18] Plotting new incremental heating $^{40}Ar/^{39}Ar$ ages (Table 2) against sample site distance from Kilauea volcano, the widely held location of the present Hawaiian hot spot, shows a linear age progression for ~1200 km between the HEB and Pearl & Hermes Atoll (Figure 2). Data from other studies using similar modern analytical methods [*Sharp and Clague*, 2006] also support this linear trend (Figure 2).

[19] The only two exceptions are the ~92 and ~82 Ma ages for samples from two volcanoes located close to Pearl and Hermes, indicating that they are part of the older Wentworth seamount chain, which intersects the Hawaiian chain [*Garcia et al*., 1987; *Pringle and Dalrymple*, 1993]. They are therefore not included in Figure 2.

[20] Extrapolating the linear age-distance relationship northward along the Emperor chain (Figure 2) fits the oldest measured ages for Kimmei, Koko [*Sharp and Clague*, 2006; *Duncan and Keller*, 2004], and Detroit [*Keller et al*., 1995] seamounts. Furthermore, $^{40}Ar/^{39}Ar$ incremental heating ages for (hawaiitic and tholeiitic) drill samples from Ōjin Seamount (located ~290 km north of Koko) [*Dalrymple et al*., 1980] fall on the same trend supporting a linear relation since at least ~57 Ma (Figure 2). While these latter ages have been measured with 1980s methods, the age spectra are in our view acceptable in light of most of the current age dating criteria such as (1) an age spectrum formed by three or more contiguous gas increments representing at least 50% of the ^{39}Ar released, (2) a well-defined isochron for the plateau points, (3) concordant isochron and plateau ages, and (4) an $^{40}Ar/^{36}Ar$ intercept on the isochron diagram not significantly different from the atmospheric value of 295.5 [*Dalrymple et al*., 1980; *Dalrymple and Garcia*, 1980]. Moreover, they are supported by a total gas age of 56.5 ± 1.3 Ma for a plagioclase mineral separate [*Sharp and Clague*, 2006] and evidence from overlying sediments and fossils indicating that Ōjin was capped by organic reefs or banks in the Paleocene to Eocene [*Jackson et al*., 1980].

[21] Similarly, $^{40}Ar/^{39}Ar$ incremental heating ages for samples dredged from Jingū Seamount [*Dalrymple and Garcia*, 1980], located ~70 km NE of Ōjin Seamount but on the same isolated volcanic structure (Figure 1), also fall on the linear trend (Figure 2). The age-distance relation therefore seems to have been surprisingly linear from at least 57 Ma until ~25 Ma (see Figure 2), covering ~1900 km in the central part of the Hawaiian-Emperor seamount chain, including the HEB. Furthermore, since this trend also predicts the ~82 Ma age [*Keller et al*., 1995] for the Detroit seamount located at the northern end of the Emperor Seamount Chain, it seems a possibility that the age-distance relation has been linear since the Late Cretaceous. However, measured ages from the waning shield or the postshield stage at Nintoku and Suiko Seamounts [*Duncan and Keller*, 2004; *Sharp and Clague*, 2006], located north of Koko and south of Detroit Seamount along the Emperor Seamount Chain are ~9 Myr younger than predicted by this linear relationship.

[22] While the linear age-distance slope discussed here provides a reasonable model, it predicts ages that are up to ~1.5 Myr too young for the arcuate part of the HEB, Koko, Helsley, Turnif, Midway, and Pearl and Hermes, because measured $^{40}Ar/^{39}Ar$ are older and thus fall above the regression line (Figure 2). These rare cases of older lavas compared to an overall age-progression trend support the suggestion that dredging and drilling does not usually access the full shield-postshield history of seamount volcanism [*Sharp and Clague*, 2006, *Koppers et al*., 2012]. Given the evidence of an ~5 Myr range in ages for the HEB bend, the ~82–76 Ma age range for Detroit seamount [*Keller et al*., 1995; *Duncan and Keller*, 2004] and following the argument of *Sharp and Clague* [2006] we simply widen the linear age-distance relation by 1.5 Myr so that it incorporates the oldest lavas along the chain, evidently not sampled in most of the Hawaiian-Emperor seamounts. This seems to best reflect the interaction between the Pacific plate and the Hawaii hot spot. Moreover, the unadjusted trend (Figure 2) is consistent with predicted formation of postshield stage 9–16 (Kammu), 23-3

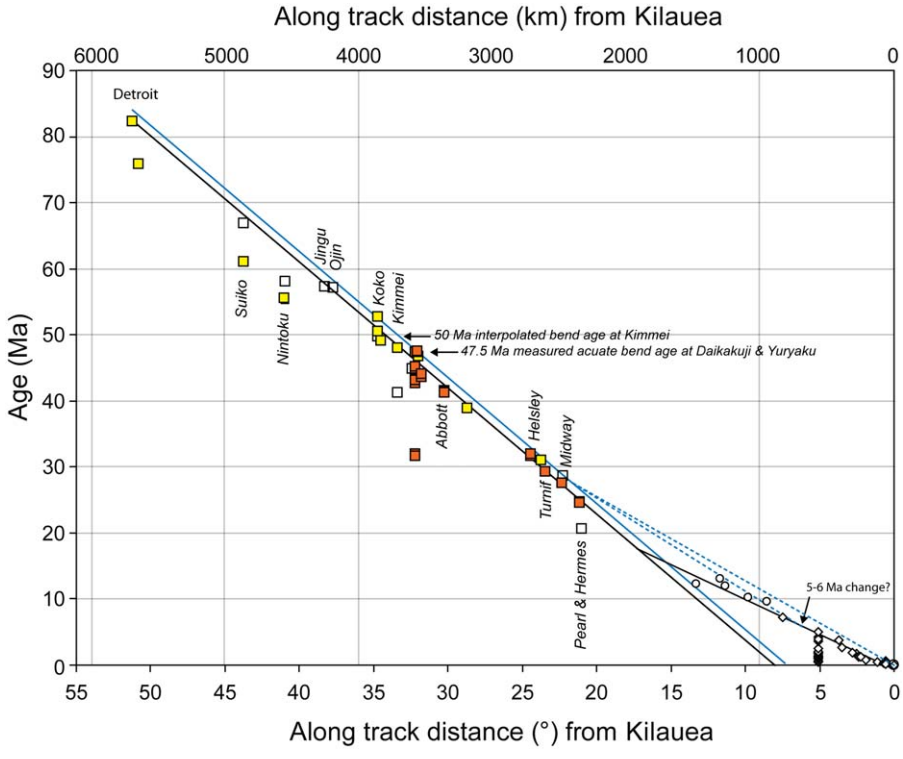

Figure 2. New (red box symbols) (Table 2) and published (yellow box symbols for post-1995 and white for pre-1995) $^{40}Ar/^{39}Ar$ isotopic ages for the Hawaiian-Emperor Seamount Chain plotted against sample site distance from Kilauea. Great circle angular distances (in degrees) along the Hawaiian chain are measured with respect to Kilauea (19.2°N, 155.05°W). Great circle distances along the Emperor track are measured with respect to the HEB (32.546°N, 187.734°W) and summed with the distance between Kilauea and the HEB. The Hawaiian-Emperor Bend is 47.5 Ma (Table 2), ~1 Myr older than the oldest existing isotopic age [*Sharp and Clague*, 2006]. Applying a regression fit to new and post-1995 $^{40}Ar/^{39}Ar$ ages and pre-1995 $^{40}Ar/^{39}Ar$ ages for Ōjin and Jingū (see text for discussion), in the same ~1900 km section of the chain (i.e., between Ōjin and Jingū and Pearl & Hermes Atoll) predicts a linear 57 ± 2 km/Myr distance versus age slope. This regression does not take into consideration the ~100 km width of the Hawaiian-Emperor chain (see Figure 1). Extrapolating this regression fit (long black line) to the old end of the Emperor Seamount Chain predicts the oldest lava ages for Detroit seamount. Extrapolation to the young end of the Hawaiian Seamount Chain (same long black line) shows that age data for the young end of the Hawaiian seamount (small white spheres) and islands (small white diamonds) chain predicts roughly a doubling in the rate of age progression to ~100 km/Myr since at least 15 Ma. The two dashed blue lines show the possibility that age progression increased to only about 80 km/Myr starting as early as 27 Ma (see text for discussion). The long narrow solid blue line shows the linear trend shifted by 1.5 Myr such that it lays above all data points, consistent with the assumption that eruptions do not occur before a plate has passed over the plume. Model ages discussed in the text are inferred from this "adjusted" (+1.5 Myr) linear fit. All ages have been calibrated to the same age standard and decay constant and are available in a recalibration database as supporting information together with references and age and geochemistry data for samples used in this study.

(Helsley), 34-1 (Pearl and Hermes), and 25-1 (Turnif Seamount) 1–2 Myr after the main shield stage (see Geochemistry section of the results).

3.2. Age of the Hawaiian-Emperor Bend

[23] The oldest measured $^{40}Ar/^{39}Ar$ ages reported here for new dredge samples from Daikakuji (47.3 ± 1.1; 47.5 ± 0.5; 47.5 ± 0.9; 47.5 ± 0.7; 47.4 ± 1.1; and 47.5 ± 0.5 Ma) and Yuryaku (47.4 ± 0.5; 47.4 ± 0.9; and 47.3 ± 0.6 Ma) seamounts (Figure 1) show that volcanism had started in the most arcuate part of the HEB by at least 47.5 Ma, about 1 Myr earlier that implied by the oldest existing (46.8 ± 0.1 Ma) isotopic age [*Sharp and Clague*, 2006]. Moreover, younger ages for Yuryaku show that volcanism continued for at least another ~5 Myr (Figure 2). Very young (~32 Ma) ages for two Yuryaku samples are discussed in section 3.4.

[24] Following a simple fluid dynamic argument given by *Griffiths and Richards* [1989], the time of plate motion change should correspond to the point on the track where the direction first changes, not the most arcuate part on the bend. *Sharp and Clague* [2006] estimate that the HEB initiated north of Daikakuji, near Kimmei seamount where the trend of the Hawaiian-Emperor Seamount Chain first starts to rotate from nearly due south to southeast (Figure 1). Because the postshield alkalic 48.0 ± 0.2 Ma basalt age for Kimmei seamount provides a minimum age estimate for the HEB, a 50.0 ± 0.9 Ma age is estimated for the HEB initiation by interpolating for Kimmei's shield formation age by fitting a trend to dated shield-stage lavas at adjacent seamounts (Koko's northern eruptive enter, Daikakuji, and Abbott seamounts) [*Sharp and Clague*, 2006]. Our linear trend predicts more robustly a 50 Ma age for the earliest initiation of the HEB (Figure 2). Recent new ages for the Louisville Seamount Chain predict that the oldest lavas at the corresponding Louisville bend formed synchronously at ~50 Ma [*Koppers et al*., 2011].

3.3. Faster Age Progression Since ≥15 Ma

[25] The measured ages for the Hawaiian-Emperor Seamount Chain reported over the last two decades have always implied an increase in the rate of age progression sometime between ~18 and 25 Ma, potentially reflecting a corresponding increase in Pacific plate motion relative to a fixed or slowly moving Hawaiian hot spot [*Clague and Dalrymple*, 1989, *Duncan and Keller*, 2004; *Andrews et al*., 2006]. An increase in the rate of age progression along the youngest section of the HESC is confirmed here by the impossibility of successfully extrapolating our linear age progression to the present hot spot and so providing strong evidence for a faster age progression along the youngest ~1500 km of the Hawaiian chain (Figure 2). Establishing when this change occurred is hindered by a roughly 1300 km wide gap in isotopic age data between Brooks Bank and Pearl & Hermes Atoll (Figure 1).

3.4. Geochemistry

[26] Volcanism on individual Hawaiian volcanoes may occur over a period of up to 6 Myr [e.g., *Clague and Dalrymple*, 1987] with the geochemistry of the erupted lavas changing systematically over the lifetime of a single volcano. During the shield stage, more than 90% of the volume of the volcano is erupted in the form of tholeiitic basalt within a period of less than about 1 Myr. The postshield stage is characterized by smaller volumes of transitional to alkalic basalt and more differentiated lavas, which are extruded at lower eruption rates over a period of around 500 kyr. The transition from shield to postshield magmatism may be gradual or may be accompanied by a brief hiatus. After a period of volcanic quiescence and erosion of up to 2 million years, very small volumes of silica-undersaturated alkalic lava may be erupted during the rejuvenated stage. The later alkalic lavas are thought to result from smaller degrees of mantle melting, after the volcano has passed over and away from the hot spot location. Over a 6 Myr period, a Hawaiian volcano would have moved by around 342 km relative to a "fixed" hot spot, assuming a 57 km/Myr age progression. In order to infer past mantle and plate motions from chronological studies of seamounts, it is therefore critical to determine the evolutionary stage to which the dated samples belong. Although the bulk of the volcano is composed of tholeiitic basalt erupted during the shield stage, dredging is likely to preferentially sample the overlying postshield and rejuvenated stage flows, which thus may be up to 6 Myr younger than the main shield phase of volcano growth. However, since the chemical composition of magmatism changes systematically during the evolution of an individual volcano, the chemistry of dredged samples from a single volcano can be used to infer their age relative to the initial shield-building stage.

[27] Major and trace element concentrations of SO141 samples dated in this study are in supporting information. The samples have undergone varying degrees of seafloor alteration, and concentrations of the more mobile elements, including Na and K, do not reflect primary magmatic concentrations. Relatively high La, Y, and Lu concentrations together with negative Ce anomalies in four of the samples (Figure 3) probably result from seafloor phosphatization. Conventional geochemical indicators, such as total alkalis and La/Sm ratios therefore cannot be used to distinguish shield from postshield samples. On the other hand, the relative concentrations of high field strength elements (Nb, Ta, Hf, Zr, Th) are unlikely to be affected by alteration processes. As a result, the systematic relationships between two high field strength elements can be reliably employed to distinguish late stage, alkalic Hawaiian lavas that have lower Zr/Nb and generally higher Nb concentrations from shield stage, tholeiitic lavas that have higher Zr/Nb and lower Nb concentrations.

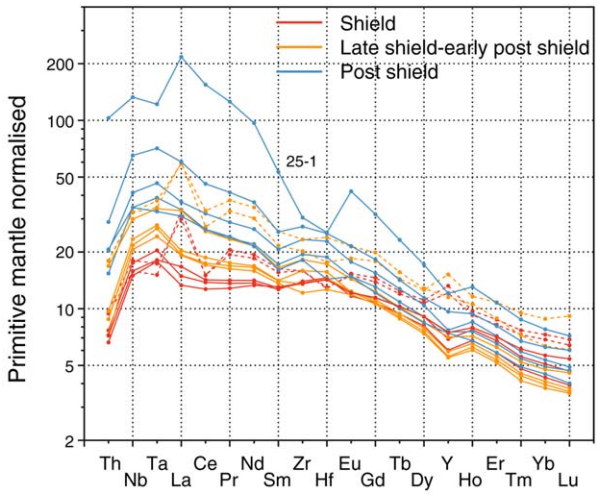

Figure 3. Primitive mantle normalized trace element data for dated SO141 samples. Elements most susceptible to seafloor alteration have been excluded, however the anomalously high La, Y, and low Ce concentrations of four of the samples (dashed lines) are likely to result from postmagmatic seafloor phosphatisation. Sample 25-1 from Turnif Seamount is enriched in the highly incompatible elements, and is a relatively evolved lava erupted during the postshield stage. Other, basaltic samples are classified as shield (red) or postshield (blue), on the basis of their Zr/Nb ratios (see text).

We have therefore been able to classify the SO141 samples on the basis of their Zr/Nb ratios.

[28] Assuming that postshield lavas have Zr/Nb < 9 (Figure 4), then samples 6-3 (Daikakuji), 9–16 (Kammu), 23-3 (Helsley), and 34-1 (Pearl and Hermes) are likely to have been erupted during the postshield stage. Sample 25-1 (Turnif Seamount) is enriched in highly incompatible elements such as Th and Nb, has low Zr/Nb, and a distinct negative Zr, Hf anomaly (Figure 3), and is an evolved lava belonging to the post-shield stage. The fact that this sample lies close to the age-progression trend in Figure 2 suggests that it is likely less than 1–2 Myr younger than the underlying shield lavas. All other SO141 Hawaiian samples are tholeiitic or transitional in composition, and these, as well as the postshield alkalic samples listed above are therefore likely to have been erupted within the first 1–2 Myr from the inception of volcanism, within the shield stage or postshield stage. On Daikakuji and Kammu Seamounts, where both late shield and postshield lavas were dated, the ages of both are similar within error.

[29] On the basis of their trace element concentrations, the two anomalously young (32 Ma) samples from Yuryaku Seamount (5–6, 5–8) are both tholeiites. These are also two of the most altered samples, as illustrated by their anomalously high La and low Ce concentrations. Similarly, young ages for Meiji and Detroit seamounts have been reported and attributed to resetting of the K-Ar system [*Duncan and Keller*, 2004]. However, it seems unlikely that variable seafloor alteration could result in identically young isotopic ages. An alternative explanation is suggested by seismic data and ash layers in ODP holes drilled in the ca. 76–81 Ma Detroit Seamount showing that volcanism was active throughout much of the Eocene (ca. 52–34 Ma), which has been attributed to possible changes in regional plate motions [*Kerr et al.*, 2005]. We speculate that the young ages of some lavas from Yuryaku Seamount reflect later, extension-related magmatism resulting from the location of this seamount close to the "bend" in the Hawaiian-Emperor chain, where intraplate extension and magmatism may have been concentrated.

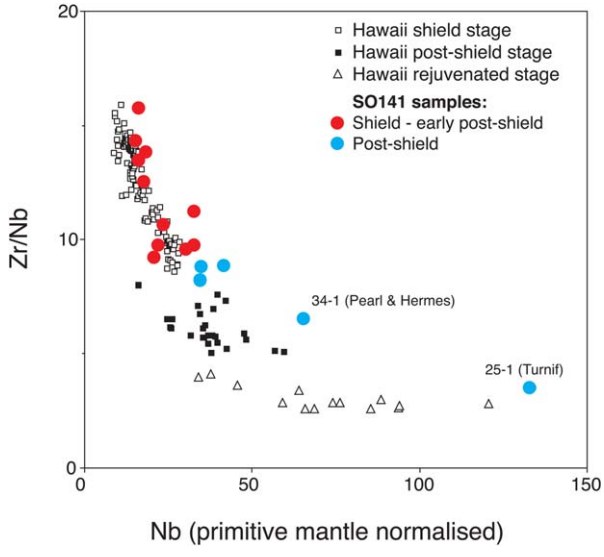

Figure 4. Variation of Zr/Nb with primitive mantle-normalized Nb (for ease of comparison with Figure 3) for SO141 samples, and lavas from different eruptive stages of Hawaiian volcanoes, showing that younger, more alkalic lavas have lower Zr/Nb ratios and higher Nb concentrations. Data for Hawaiian shield tholeiites from Koolau [*Huang and Frey*, 2005] and Kilauea [*Pietruszka and Garcia*, 1999], postshield alkalic lavas from Nintoku Seamount [*Shafer et al.*, 2005], and rejuvenated volcanics from Koolau [*Yang et al.*, 2003] shown for comparison. On the basis of this diagram, we have classified basaltic SO141 samples with Zr/Nb > 9 as shield stage lavas, and samples with Zr/Nb < 5 as rejuvenated lavas. Sample 25–1 from Turnif Seamount is a highly evolved lava belonging to the late post-shield stage.

[30] We note that the trace element composition of sample 37-1 (Bank 9 Seamount) is indistinguishable from that of Hawaiian tholeiites (not shown), despite its much older age, which indicates that this seamount is part of the Wentworth seamount chain. Therefore, not all lavas with Hawaiian-like chemistry from seamounts along the Hawaiian chain were necessarily erupted above the Hawaiian hot spot.

4. Discussion

4.1. Hawaiian and Louisville Hot Spot Relative Motion Since 80 Ma

[31] Observed long-term variations along seamount trails, such as the Hawaiian-Emperor and Louisville seamount trails, are now starting to be used to effectively calibrate and test mantle flow simulations, in particular by using state-of-the-art paleolatitude and $^{40}Ar/^{39}Ar$ age data to provide key boundary conditions [*Steinberger*, 2000; *Steinberger and O'Connell*, 2000; *Tarduno et al*., 2003; *Steinberger et al*., 2004; *Koppers et al*., 2004; *Tarduno*, 2007; *Tarduno et al*., 2009, *Koppers et al*., 2012].

[32] The Louisville Seamount Chain is the only South Pacific counterpart to the Hawaiian-Emperor Seamount Seamount Chain, which records the same ~80 Myr period of copolar Pacific plate motion [*Hawkins et al*., 1987; *Lonsdale*, 1988; *Watts et al*., 1988; *Courtillot et al*., 2003; *Koppers et al*., 2004, 2011, 2012] and so the age progressions along these two primary Pacific seamount chains can be used to establish the relative motions between the Hawaii and Louisville hot spots over this period [e.g., *Wessel et al*., 2006; *Wessel and Kroenke*, 2008, 2009]. Only if the Hawaii and Louisville hot spots were fixed relative to each other by remaining stationary or by moving in unison since the Late Cretaceous, would the great circle separation between seamounts of similar age on these two trails (using the oldest volcano shield lavas sampled and age dated) have remained constant [e.g., *Wessel et al*., 2006; *Wessel and Kroenke*, 2008, 2009].

[33] Current assessment of interchain great circle distances using directly dated sample sites of similar age on the Hawaiian-Emperor and Louisville chains [*Clague and Dalrymple*, 1989; *Duncan and Keller*, 2004; *Koppers et al*., 2004; *Sharp and Clague*, 2006] shows no significant variations after ~55 Ma, when there was an abrupt 2° change in inferred interchain distance [*Wessel and Kroenke*, 2009]. But prior to 55 Ma, the age records show that interchain separation was 278 km larger at ~61 Ma and 556 km larger at 81 Ma (between Detroit and Osbourn volcanoes) [*Wessel et al*., 2006; *Wessel and Kroenke*, 2008, 2009]. This implies either that both the Hawaiian and Louisville hot spots were fixed sometime after ~55 Ma or that they were moving with the same speed and direction. Before ~55 Ma at least one or both must have been experiencing some independent motion. Paleolatitude data [*Tarduno et al*., 2003] show that the Hawaiian hot spot drifted southward until about 47 Ma. Therefore, the lack of evidence for significant latitudinal motion of the Louisville hot spot between 70 and 50 Ma [*Koppers et al*., 2012] suggests that the changes in Louisville-Hawaii hot spot separation results from independent motion of the Hawaiian hot spot. The changing hot spot separation is qualitatively consistent with hot spot drift predicted by models of past mantle circulation and the southern paleolatitude shift in the Emperor Seamount Chain [*Steinberger*, 2000; *Tarduno et al*., 2003; *Koppers et al*., 2004; *Wessel and Kroenke*, 2008]. The Emperor paleolatitude data may also (partially) reflect true polar wander (TPW), so they do not necessarily require that southward motion of the Hawaiian hot spot continued until the time of the HEB. However, TPW would result in an apparent southward drift of the Louisville hot spot, which is not evident in the paleomagnetic data for Louisville lavas.

4.2. Implications for Hawaiian Hot Spot Motion and Bend Formation

[34] With our new data, we can now identify finer-scale changes in current estimates of relative motion between the Hawaii and Louisville hot spots, as discussed in the previous sections, and evaluate different combinations of linear (this study) and nonlinear age progression models [e.g., *Duncan and Keller*, 2004; *Sharp and Clague*, 2006] (Figure 5 and 7). We will be able to investigate also whether an unchanged or faster age progression since 15 Ma provides a better explanation for the largely unconstrained young part of the Louisville age record. The results of these evaluations will in turn allow us to relate potential periods of change in interchain motions (due to mantle flow) to regional or more global plate-driving forces.

[35] Assuming that age progression in both the Hawaiian-Emperor (Figure 2) and Louisville

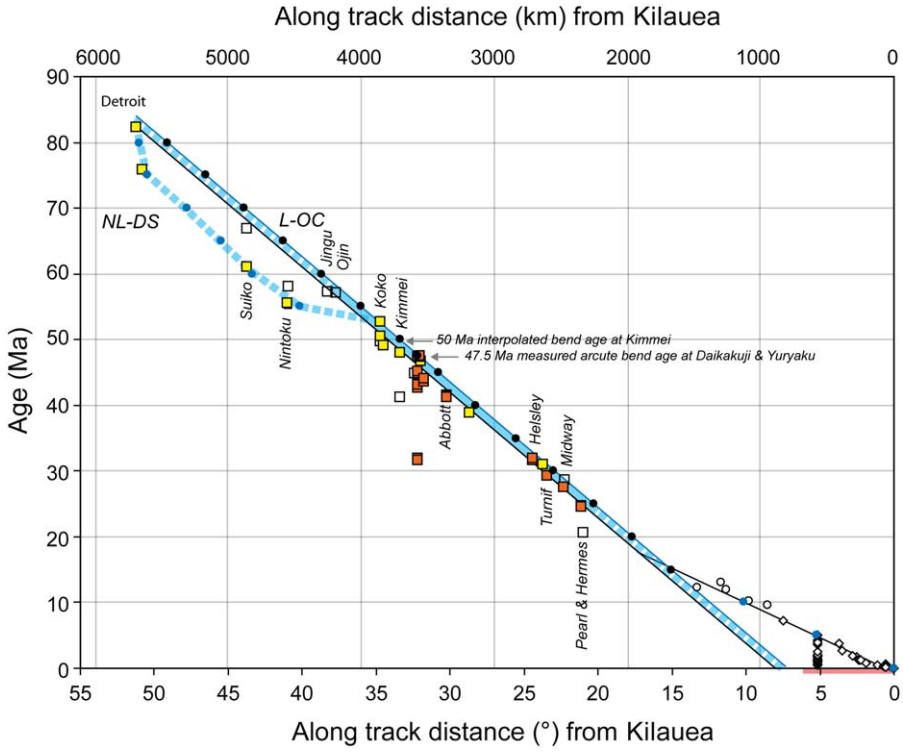

Figure 5. The long thick blue line is for the linear age-distance relation for the central 1900 km of the HESC in Figure 2. Extrapolation of linear trend to the old end of the Emperor Seamount Chain (dashed line) predicts the oldest lava ages for Detroit seamount. Including this measured Detroit age in the regression (Figure 2) predicts the same result. The L-OC model assumes that age progression in both the Hawaiian-Emperor and Louisville seamount chains [*Koppers et al*., 2011, 2012] has been linear to a first-order approximation since at least 82 Ma (Figures 5 and 7). The NL-DS model assumes nonlinear age progression in the HESC based on *Duncan and Keller* [2004] and *Sharp and Clague* [2006]. Filled circles show interpolated volcanic propagation in 5 Myr increments inferred from age-distance relations: black circles are for linear L-OC and blue circles are for nonlinear NL-DS and faster propagation since ≥15 Ma. Red bar is for the recently discovered upper-mantle low-velocity anomaly elongated in the direction of the island chain [*Wolfe et al*., 2009]. Unchanged age progression since ≥15 Ma predicts that the present location of the Hawaiian hot spot is at the NW side of this velocity anomaly. Shown also are measured arcuate 47.5 Ma (this study) and interpolated ~50 Ma initiation [*Sharp and Clague*, 2006; *Garcia et al.,* 2013; this study] ages for the HEB. Location coordinates for linear L-OC and nonlinear NL-DS age-distance relations are in Table 3. Other details as for Figure 2.

seamount chains (Figures 6 and 7) has been linear since at least 82 Ma (L-OC Model) implies an overall decrease in hot spot separation of ~334 km (3°) between ~80 Ma and ~47.5 Ma at a constant rate of ~10 km/Myr (Figure 8a and Table 3). However, current palaeontological age estimates for sediments recovered at the bottom of IODP Leg 330 drill sites on Louisville seem to be as much as 4 Myr older than the $^{40}Ar/^{39}Ar$ ages for the underlying lavas [*Koppers et al*., 2012] (Figure 7). Our new estimate of ~334 km (3°) for the overall decrease in separation is roughly half that implied by other recent estimates already discussed [*Wessel et al*., 2006; *Wessel and Kroenke*, 2008, 2009]. Furthermore, since ~55 Ma a constant overall hot spot separation (~8200 ± 75 km) has been maintained, which has continued until ≥15 Ma, and possibly to the present.

[36] However, nonlinear age progression can also be inferred from existing age data for the Emperor Seamount Chain for the period 82–50 Ma based on *Duncan and Keller* [2004] and *Sharp and Clague* [2006] (referred to here as the nonlinear NL-DS model). Assuming a linear age-distance relationship for Louisville (L-OC) together with a nonlinear age-distance relation for the Hawaiian-Emperor chain (NL-DS) predicts a doubling of overall hot spot motion since ~75 Ma to ~719 km (6.5°) (Figure 9). Again a hot spot speed of ~10 km/Myr is predicted until 55 Ma with much faster hot spot speed between ~55 Ma and 50 Ma (~101 km/Myr) (Figure 9).

Table 3. Interchain Separation Between the H-E and LOU Seamount Chains

Stage (Ma)	Separation (km)	LOU Latitude	LOU Longitude	H-E Latitude	H-E Longitude
		Linear LOU		*Linear H-E*	
80	8472	−25.75	−175.13	49.30	168.40
75	8423	−27.76	−174.08	46.80	169.40
70	8379	−29.85	−173.24	44.30	170.34
65	8320	−31.80	−172.10	41.60	170.50
60	8282	−33.89	−171.27	39.00	170.70
55	8228	−35.90	−170.17	36.37	171.28
50	8176	−37.88	−168.78	33.65	171.60
47.5	8142	−38.64	−167.84	32.50	172.20
45	8156	−39.56	−166.92	31.85	173.70
40	8184	−41.06	−164.95	30.80	176.40
35	8207	−42.52	−162.69	29.70	179.30
30	8210	−44.05	−160.49	28.30	−178.10
25	8223	−45.25	−157.87	27.25	−175.39
20	8233	−46.41	−155.19	26.20	−172.70
15	8227	−47.24	−152.25	25.30	−169.90
10	8126	−48.33	−149.32	23.70	−164.80
5	8021	−49.30	−146.38	22.13	−159.69
0	7789	−50.35	−143.34	19.20	−155.05
		Fast LOU		*Linear H-E*	
10	8233	−48.97	−147.37	23.70	−164.80
5	8243	−50.70	−142.45	22.13	−159.69
0	8118	−52.40	−137.20	19.20	−155.05
		Linear LOU		*Nonlinear H-E*	
80	8683	−25.75	−175.13	51.15	167.70
75	8861	−27.76	−174.08	50.60	167.80
70	8805	−29.85	−173.24	48.00	168.90
65	8782	−31.80	−172.10	45.75	169.70
60	8789	−33.89	−171.27	43.70	170.50
55	8683	−35.90	−170.17	40.50	170.72

Linear LOU: Linear age progression for Louisville chain; Louisville hot spot at 50.5°S; 143°W (black circles in Figures 6 and 7).
Fast LOU: Faster age progression for Louisville chain since 15 Ma; Louisville hot spot at 52.4°S, 137.2°W (blue circles in Figures 6 and 7).
Linear H-E: Linear age progression for Hawaii-Emperor before 15 Ma (black circles in Figure 5).
Nonlinear H-E: Linear age progression for Hawaii-Emperor before 15 Ma (blue circles in Figure 5).
Fast age progression since 15 Ma is assumed in all cases for Hawaii-Emperor (Figure 2).

[37] Our predicted overall amount and speed of Hawaiian hot spot motion during formation of the Emperor Seamount Chain can therefore potentially range from being much less/slower than to roughly comparable (within analytical uncertainty) to the estimates of Hawaiian hot spot motion based on the paleolatitude prediction of roughly ∼11 to 13° (∼1222 to 1445 km) of motion at ∼40 and 50 ± 11 (1σ) km/Myr between ∼80 Ma and 47 Ma [*Tarduno et al*. 2003]. Similarly, numerical models of plumes in a convecting mantle by *Steinberger et al*. [2004] and *Doubrovine et al*. [2012] also predict several 100 km southward motion of the Hawaiian plume relative to Louisville ending around 30 Ma (Figure 9).

[38] An important implication is that there is significantly better agreement between independent numerical models of past mantle circulation [*Steinberger et al*., 2004, red line in Figure 8; *Doubrovine et al*. 2012, gray line] with hot spot relative motion predicted by linear L-OC age-distance relations compared to those involving a nonlinear age-distant relation for Hawaii-Emperor (Figure 9). The implications of these findings are further discussed below.

4.3. Implication for Hot Spot Motion or Migrating Spreading Ridges

[39] It is striking that the older isotopic ages for Detroit (Figure 2) and Osbourn [*Koppers et al*., 2011, 2012] (Figure 7) seamounts both lie on an extension of the linear age progression defined by younger samples from the same seamount chain. Applying a linear age-distance relation also results in interchain separation distances that require less hot spot drift during formation of the Emperor Seamount Chain to make it compatible with the older isotopic age for Detroit seamount (∼82 Ma).

[40] However, it is likely that Detroit Seamount formed at the Kula-Pacific spreading ridge while

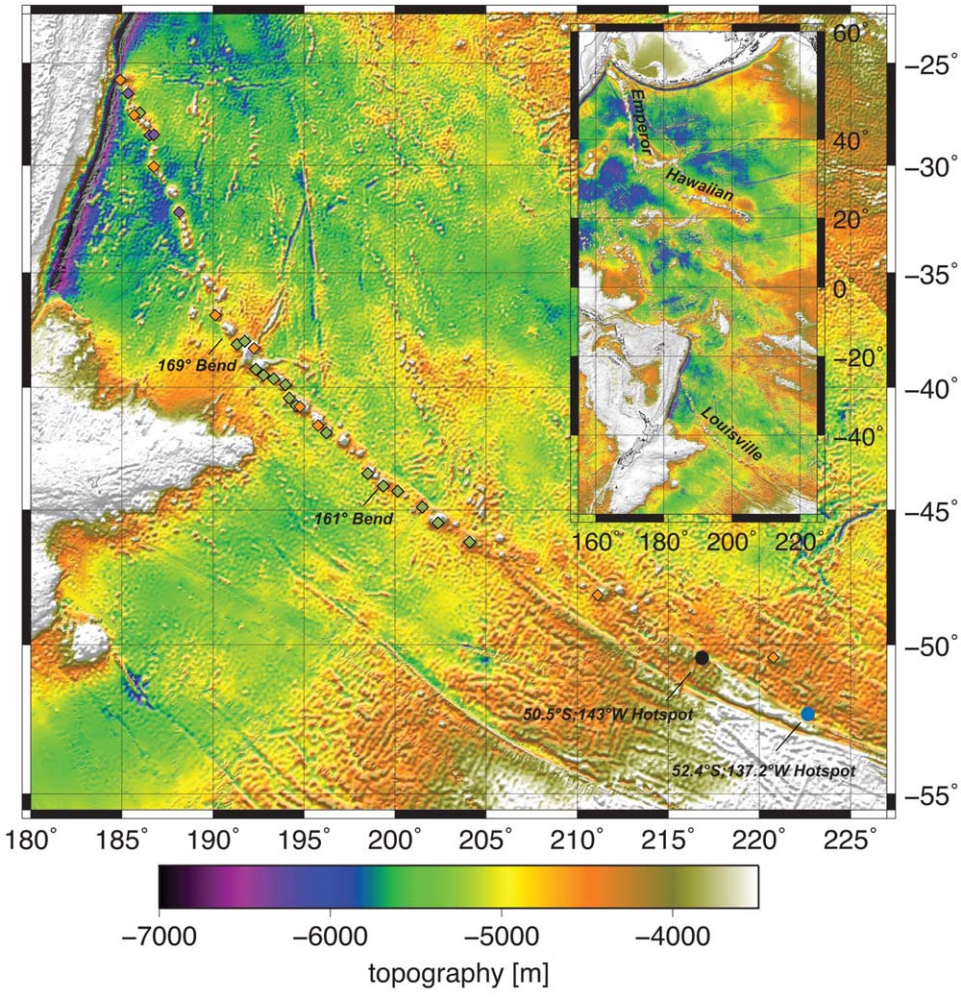

Figure 6. Topography map [*Smith and Sandwell*, 1997] of the Louisville Seamount Chain created with GMT software [*Wessel and Smith*, 1991]. Symbols are for locations of cited sample ages. See Figure 7 for sources and other details.

the hot spot was still north of the ridge and that ridge overrode the Hawaiian hot spot at ~78 Ma, such that the younger ~76 Ma Detroit lava ages in fact are a better representation of eruption directly above the hot spot [*Steinberger and Gaina*, 2007]. A near-ridge origin for Detroit Seamount is supported by the depleted trace element and isotopic compositions of Detroit lavas, which changed drastically over this 6 Myr period. The oldest 82 Ma ODP Site 884 lavas have the most depleted compositions approaching those of Pacific mid-ocean ridge basalt [*Keller et al*., 2000; *Regelous et al*., 2003], whereas younger Detroit lavas from ODP Sites 883 and 1203 have less extreme compositions, but are nevertheless more depleted than those of all other Hawaiian lavas, consistent with melting off axis, beneath young, thin oceanic lithosphere at 76 Ma [*Huang et al*., 2005; *Frey et al*., 2005]. Moreover, the only part of the Emperor Chain that is smooth, almost isostatically compensated and hence almost not visible in the gravity image, indicating that it erupted on a spreading ridge, is between Detroit and Meiji seamounts. In contrast, the isolated seamounts south of Detroit are clearly visible on the gravity map and hence not isostatically compensated having been loaded on top of already slightly matured ocean crust [*Steinberger and Gaina*, 2007]. A possible explanation for such faster drift during the time period ~81–47 Ma is a hot spot "capture-and-release" scenario [*Tarduno et al*., 2009]. This scenario assumes migration of the Kula-Pacific spreading ridge away from the hot spot after 81 Ma such that thereafter the hot spot drifts rapidly southward to regain its equilibrium position in the mantle by ~47 Ma [*Tarduno et al*., 2009].

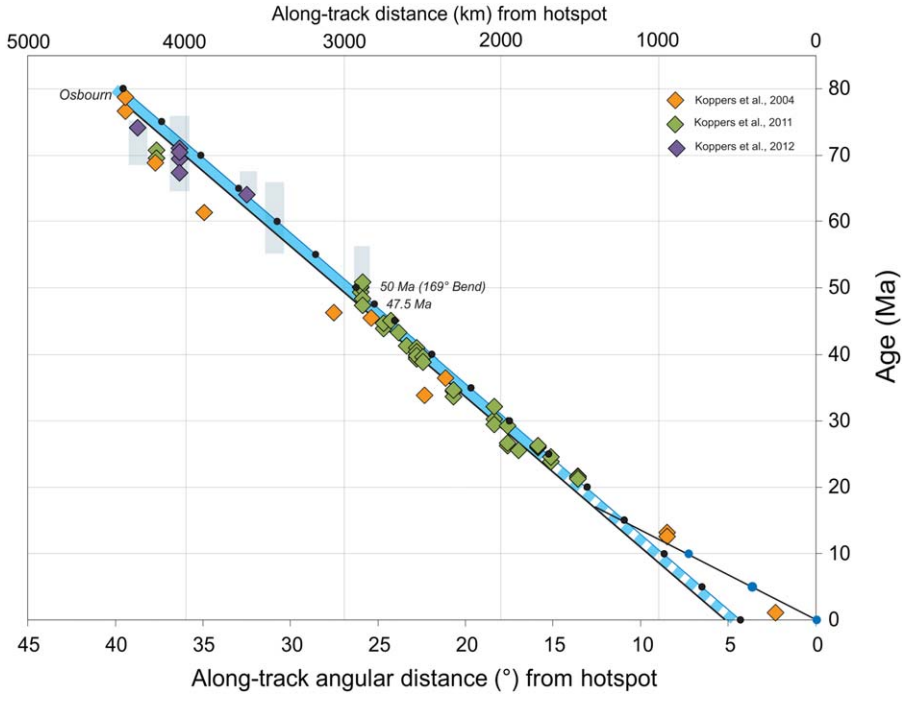

Figure 7. $^{40}Ar/^{39}$ages for samples dredged [*Koppers et al*., 2004, 2011] and drilled [*Koppers et al*., 2012] from the Louisville Seamount Chain (Figure 6) plotted against sample site distance. Distances are great circle angular distances (in degrees) measured along the seamount trail, with respect to the 52.4°S and 137.2°W hot spot location [*Wessel et al*., 2006; *Wessel and Kroenke*, 2008] using a "young" (43.95°S, 160.6°W) and an "old" (37.6°S, 169.1°W) bend in the seamount morphology as described in Figure 2. The long black line is a visual best fit to the age data that predicts a linear ~48 km/Myr distance versus age slope. The thick blue line is for a 1.5 Myr "adjustment" to this linear age distance fit as applied to the Hawaii-Emperor Seamount Chain in Figure 2. Model ages discussed in the text are inferred from this "adjusted" linear fit. Black circles show interpolated volcanic propagation in 5 Myr increments along the Louisville hot spot trail inferred from linear L-OC (Table 3). Note that the linear age-distance relation—L-OC—predicts that the present Louisville hot spot is located at 50.5°S; 143°W. Blue circles are for inferred faster propagation in the Louisville chain since at least 15 Ma relative to the assumed location used for the Louisville hot spot at 52.4°S; 137.2°W [*Wessel et al*., 2006; *Wessel and Kroenke*, 2008]. Gray rectangles are current best estimates for palaeontological ages for sediments just above basement lavas in IODP Leg 330 drill sites [*Koppers et al*., 2012].

4.4. Implications for Major Changes in Pacific Tectonics and Mantle Flow

[41] Tectonic plate reorganization in the Pacific was triggered by the subduction of the Izanagi-Pacific ridge (IP) ~60–55 Ma. This was followed by initiation of the Marianas/Tonga-Kermadec subduction zone between 53 and 50 Ma [*Whittaker et al*., 2007a; *Sharp and Clague*, 2006; *Tarduno et al*., 2009]. Our confirmation of a ~50 Ma earliest initiation age for the HEB [*Sharp and Clague*, 2006; *Garcia et al*., 2013] points to synchronicity with 53–50 Ma Marianas/Tonga-Kermadec subduction initiation [*Whittaker et al*., 2007a; *Sharp and Clague*, 2006; *Tarduno et al*., 2009]. Moreover, once the Izanagi-Pacific ridge had been subducted by ~55 Ma forces acting on the Pacific plate changed such that the Pacific absolute plate motions switched [*Whittaker et al*., 2007a, 2007b].

[42] A change in hot spot relative motion between ~55 and 50 Ma (Figures 8 and 9) is therefore roughly synchronous with completion of IP subduction, Marianas/Tonga-Kermadec subduction, and a change in Pacific plate motion at that time [*Sharp and Clague*, 2006; *Whittaker et al*., 2007a, 2007b].

[43] Furthermore, there seems to be a rough coincidence with a major physical gap in the Emperor Seamount Chain starting between Nintoku and Jingu seamounts indicating a decrease in overall volcanism (Figure 1). If this "gap" is related to a rapid change in plume motion between 55 and 50

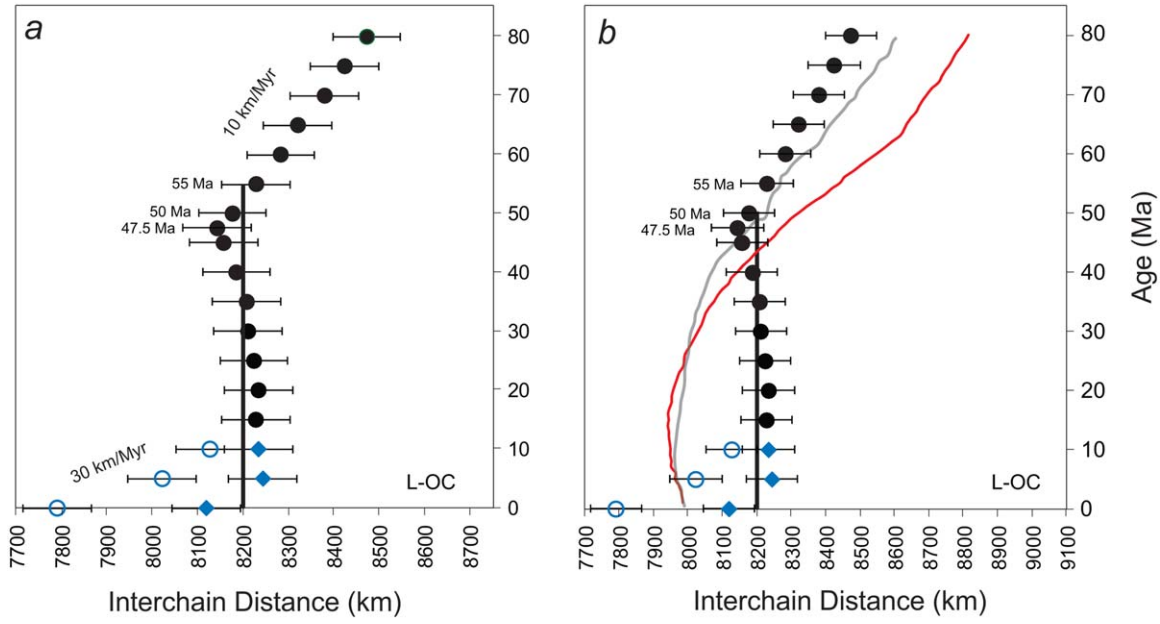

Figure 8. Interchain separation between coeval locations on the Hawaiian-Emperor and Louisville seamount chains in 5 Myr increments assuming linear age-distance relations on both chains. (a) Black circles are for hot spot separation inferred from linear age-distance relations for Hawaiian-Emperor (Figure 5) and Louisville (Figure 7) since 80 Ma. L-OC predicts an overall decrease in hot spot separation of ~334 km (3°) between ~80 Ma and ~47.5 Ma at an average rate of ~10 km/Myr. A constant mean separation (indicated by vertical black line) of ~8200 ± 75 km was maintained roughly from 55 Ma until ≤15 Ma, and maybe to the present. Blue diamonds are for interchain separation predicted by assuming faster age progression in both chains since 15 Ma, and blue circles are for faster age progression only for Hawaiian-Emperor. Errors bars allow for widths of seamount trails. Other details as for Figures 5, 7, and Table 3. The error bars are for a fixed uncertainty of ±75 km for the ~100 km and ~50 km widths of the Hawaiian-Emperor and Louisville chains. (b) Same as Figure 8a with the addition of the relation between hot spot relative motion predicted by linear L-OC age-distance relations and numerical models of past mantle circulation *Steinberger et al*. [2004] (red line) and *Doubrovine et al*. [2012] (gray line). A conversion 111.12 km = 1° is used.

Ma it would fit with measured age of ~55 Ma for Nintoku, which is similar to that of Jingu, and about 10 Ma younger than the ~65 Ma age predicted by a linear age-distance relation (Figure 5).

4.5. Faster Age Progression Since Between 15 and 27 Ma

[44] A major increase in the rate of age progression is seemingly required to explain the relatively numerous isotopic ages for the well-sampled Hawaiian Islands (Figure 2). An increase in Pacific plate motion at ~15 Ma to ~100 km/Myr might have resulted from a plate motion change around 17–14 Ma predicted by *Wessel and Kroenke* [2008] in their reconstruction of Pacific plate motion relative to 12 hot spot chains that, as they discuss, correlates with numerous tectonic events around the Pacific, including subduction of the Marcus-Necker ridge [e.g., *Miller et al*., 2006], rapid extension in the Basin and Range province [e.g., *Dilles and Gans*, 1995], and transrotation in the Los Angeles Basin [e.g., *Ingersoll and Rumelhart*, 1999].

[45] However, the gap in age information for the younger Hawaiian seamounts and atolls allows for the possibility that the increased age progression was roughly only about 80 km/Myr starting as early as 27 Ma and (Figure 2), which would agree with the major Pacific-wide modeled change in age progression [*Wessel and Kroenke*, 2008] presumably reflecting the Farallon plate breakup [*Wessel and Kroenke*, 2008, *and references therein*]. Furthermore, new models of Pacific absolute plate motion relative to hot spots and models of relative plate motion involving the Pacific plate all agree there was a significant change in the late Neogene (Chron 3A, ~5.9 Ma), reflecting a more northerly absolute motion than previously determined [*Wessel and Kroenke*, 2007].

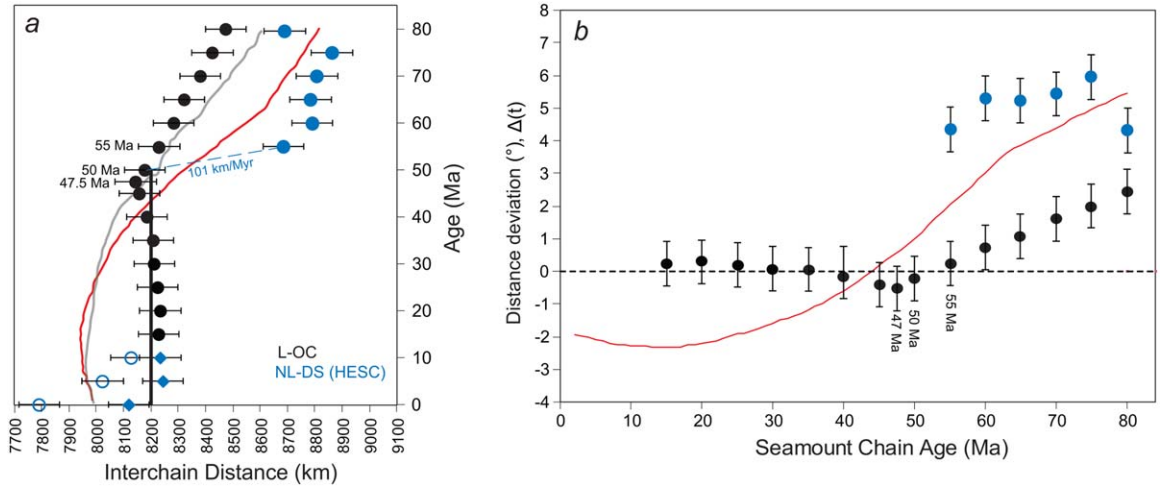

Figure 9. (a) Similar to Figure 8 with addition of interchain separation predicted by a nonlinear NL-DS age-distance relation for Hawaiian-Emperor (Figure 5) and linear L-OC relation for Louisville Seamount Chain (blue filled circles) (Figure 7). Using NL-DS for Hawaiian-Emperor implies overall hot spot motion of as much as ~719 km (6.5°) between ~75 and 47.5 Ma, and rapid motion between ~55 and 50 Ma as fast as ~101 km/Myr. (b) Difference (in distance, $\Delta(t)$) [e.g., *Wessel and Kroenke*, 2009] between hot spot separation and inferred constant mean hot spot separation of 8200 km. Other details as in Figure 8 and Table 3.

[46] The cause for this increase in Pacific plate motion may be related to increased mountain growth in the Andes that could have increased friction along the subduction zone and accordingly has been suggested to have resulted in a slowdown in convergence and Nazca plate motion [*Iaffaldano et al.*, 2006, 2007]. India's convergence rate with Eurasia also slowed down by more than 40% between 20 and 10 Ma [*Molnar and Stock*, 2009], but it is not clear whether there is a causal link to the apparent increase in Pacific plate motion.

[47] Determining whether there is a corresponding increase in age progression in the Louisville Seamount Chain is hindered by a lack of samples/ages and the virtual disappearance of the Louisville chain, which is generally attributed to a major reduction in the activity of the Louisville hot spot since about 20 Ma [*Watts et al.*, 1988; *Lonsdale*, 1988; *Koppers et al.*, 2004, 2011]. The Louisville age record, even though very sparse in data points toward the young end, can be interpreted on the basis of extrapolating the 48 km/Ma age distance trend to a Louisville hot spot currently at 50.5°S; 143°W (Figure 7). If so, then the Hawaii-Louisville hot spot separation decreased ~100 km by 10 Ma, ~200 km by 5 Ma, and ~400 km at present (Figure 8b).

[48] Assuming however that the Louisville hot spot is at 52.4°S; 137.2°W [*Wessel et al.*, 2006; *Wessel and Kroenke*, 2008] predicts a faster ~80 km/Myr Louisville age progression (Figure 7) in line with what is found on the Hawaiian Islands and resulting in virtually no change in separation by 5 Ma, and a decrease of ~100 km between the present hot spots (Figure 8). This decrease corresponds to the controversial ~5 Ma bend in the Hawaiian hot spot chain, probably representing a change in plate motion [*Cox and Engebretson*, 1985; *Cande et al.*, 1995; *Wessel and Kroenke*, 2007]. This ~5 Ma bend however is not observed in the Louisville hot spot chain, simply because the hot spot was not active at that time. Such a bend would probably eliminate this change in separation distance and imply that the present-day location of the Louisville hot spot is closer to the PAC-ANT spreading ridge. This would in turn help explain the disappearance of the Louisville chain in terms of eastward sublithospheric flow of buoyant Louisville plume material to the spreading ridge [e.g., *Sleep*, 1996].

[49] While it is not possible to distinguish between these possibilities based on existing information, the Louisville age record is not inconsistent with an increase in Pacific Plate motion at ~15–27 Ma (Figure 2). Such faster Pacific plate motion coincides with a significant decrease in volcanism on the Louisville chain and (faster) relocation of the PAC-ANT spreading ridge toward the Louisville hot spot by asymmetric spreading [*Müller et al.*, 2008], as reflected in the increasing offset in spreading anomalies north and south of the Tharp and Heezen Fracture Zones [*Small*, 1995].

Obliquely orientated aseismic ridges (e.g., Hollister) and gravity lineaments between the ridge and the hot spot suggest that this may be caused by increased asthenospheric flux from the Louisville hot spot [*Small*, 1995]. This notion is supported by major/trace element and isotopic data suggesting some interaction occurred between the Pacific-Antarctic Ridge and the mantle source for the Hollister Ridge [*Vlastélic et al*., 1998; *Vlastélic and Dosso*, 2005]. As the PAC-ANT spreading ridge migrated closer to the hot spot, it would be increasingly influenced by shallower asthenosphere flow from the hot spot that has "ponded" at sublithospheric depths and tends to flow laterally toward the spreading ridge [*Sleep*, 1996; *Tarduno et al*., 2009]. This implies the possibility of a more complex interplay between faster Pacific plate motion and hot spot-spreading ridge interaction similar to that at the Foundation Seamount Chain [*O'Connor et al*., 1998, 2001].

[50] We consider the alternative possibility of faster flow in the Pacific upper mantle for the past ~15–27 Ma, and hence faster hot spot motion, an unlikely scenario as there is no known evidence suggesting any mechanism that could drive such a basin-wide change in mantle flow rate at that time.

5. Summary and Conclusions

[51] Replicated $^{40}Ar/^{39}Ar$ incremental heating ages for 18 new samples dredged from 10 volcanoes in the central ~1200 km of the Hawaiian-Emperor Seamount Chain show that volcanism initiated in the Hawaiian-Emperor Bend at least by 47.5 Ma, ~1 Myr earlier than implied by the oldest existing isotopic age [*Sharp and Clague*, 2006], and that it continued for at least another ~5 Myr. New and existing $^{40}Ar/^{39}Ar$ ages [*Sharp and Clague*, 2006; *Duncan and Keller*, 2004; *Dalrymple et al*., 1980; *Dalrymple and Garcia*, 1980; *Clague and Dalrymple*, 1989] show a surprisingly constant ~57 km/Myr rate of age progression between at least ≥57 Ma until ≤25 Ma. Extrapolating this trend to the active Hawaiian hot spot at Kilauea volcano predicts that the rate of volcanic propagation almost doubled as recently as ~15 Ma and possibly increased as early as 27 Ma. Extrapolating the linear age progression to the old end of the Emperor Seamount Chain predicts the oldest (~82 Ma) isotopic age for Detroit seamount [*Keller et al*., 1995] and implies the possibility that the linear age-distance relation extends back to the Late Cretaceous.

[52] The possibility of a linear rather than nonlinear age-distance relation for the older part of the Hawaii-Emperor Seamount Chain has important implications for estimates of great-circle distance between coeval locations in the Hawaiian and Louisville hot spot trails. Linear age-distance relations for both the Hawaii-Emperor and Louisville seamount chains predict overall hot spot relative motion of ~334 km (3°) between ~80 Ma and ~47.5 Ma at a speed of ~10 km/Myr. Applying the assumption of nonlinear age-distance relation for the older HESC predicts overall hot spot motion of as much as ~719 km (6.5°) between ~75 and 47.5 Ma, and rapid motion between ~55 and 50 Ma as fast as ~101 km/Myr.

[53] Our new data therefore predict, within analytical uncertainty, hot spot relative motion that is much less/slower or roughly the same as indicated by the paleolatitude trend (~11–13° total motion during ~30 Myr) [*Tarduno et al*., 2003]. However, independent numerical models of past mantle circulation [*Steinberger et al*., 2004; *Doubrovine et al*., 2012] predict hot spot relative motion compatible with our linear L-OC age-distance relations (Figures 8 and 9).

[54] Change in the hot spot relative motion between ~55 and 50 Ma is broadly synchronous with the 53–50 Ma Marianas/Tonga-Kermadec subduction zone initiation [*Whittaker et al*., 2007a, 2007b], the earliest initiation of the HEB at ~50 Ma (Figure 2)[*Sharp and Clague*, 2006; *Garcia et al*., 2013] and change in Pacific plate motion from northnorthwest to westnorthwest [*Whittaker et al*., 2007a, 2007b]. Subduction of the Pacific-Izanagi ridge and demise of the Izanagi plate 60–55 Ma is a potential driving force for this series of mantle and tectonic events [*Whittaker et al*., 2007a, 2007b] that ended with completion of the arcuate HEB 47.5 Ma. The HEB appears therefore to reflect a combination of plate motion and mantle flow changes driven by the same plate/mantle reorganization. Our findings also indicate that finer scale sampling of key sections of the Emperor and Louisville seamount chains will be required to effectively calibrate and test mantle flow simulations and establish the viability of a deep earth reference frame.

Acknowledgments

[55] We thank the captain and crew of the R/V Sonne and all members of the SO141 Expedition scientific party for a successful sampling expedition. E. Flueh, J. Phipps Morgan, and W. Weinrabe helped in designing this project and carrying

out the research cruise. We are very grateful to reviewers Paul Wessel and Conall Mac Niocaill, as well as Associate Editor Anthony Watts and Mike Garcia, for their constructive comments and suggestions. R. van Elsas and I. Dold assisted with mineral separations. T. Worthington provided assistance with the geochemical analyses. M. Gowen and L. Colwell kindly shared their Excel macro for calculation age-distance relations along bending seamount chain. This work was supported by the German Ministry for Development and Research (BMBF) and the Netherlands Organization for Scientific Research (NWO).

References

Ackermand et al. (1999), Cruise Report SONNE 141, HULA 1 Expedition, Rep. 8, Inst. for Geosci., Univ. of Kiel.

Anderson, D. L. (2000), The thermal state of the upper mantle; No role for mantle plumes, *Geophys. Res. Lett.*, *27*, 3623–3626.

Andrews, D. L., R. G. Gordon, and B. C. Horner-Johnson (2006), Uncertainties in plate reconstructions relative to the hotspots; Pacific-hotspot rotations and uncertainties for the past 68 million years, *Geophys. J. Int.*, *166*, 939–951.

Cande, S. C., C. A. Raymond, J. Stock, and W. F. Haxby (1995), Geophysics of the Pitman fracture zone and Pacific-Antarctic plate motions during the Cenozoic, *Science*, *270*, 947–953.

Clague, D. A., and G. B. Dalrymple (1987), The Hawaiian-Emperor volcanic chain, *U.S. Geol. Surv. Prof. Pap.*, *1350*, 5–54.

Clague, D. A., and G. B. Dalrymple (1989), Tectonics, geochronology, and origin of the Hawaiian-Emperor volcanic chain, in *The Geology of North America, The Eastern Pacific and Hawaii, Decade of North American Geology*, edited by E. L. Winterer, et al., vol. N, pp. 188–217, Geol. Soc. Am., Boulder, Colo.

Courtillot, V., A. Davaille, J. Besse, and J. Stock (2003), Three distinct types of hotspots in the Earth's mantle, *Earth Planet. Sci. Lett.*, *205*, 295–308.

Cox, A., and D. Engebretson (1985), Change in motion of the Pacific plate at 5 Ma BP, *Nature*, *313*, 472–474, doi:10.1038/313472a0.

Dalrymple, G. B., D. A. Clague, and M. A. Lanphere (1977), Revised age for Midway volcano, Hawaiian volcanic chain, *Earth Planet Sci. Lett.*, *37*, 107–116.

Dalrymple, G. B., M. A. Lanphere, and D. A. Clague (1980), Conventional and 40Ar/39Ar K-Ar ages of volcanic rocks from Ōjin (Site 430), Nintoku (Site 432), and Suiko (Site 433) seamounts and the chronology of volcanic propagation along the Hawaiian-Emperor Chain, *Initial Rep. Deep Sea Drill. Proj*., vol. *55*, pp. 685–693, U.S. Gov. Print. Off., Washington, D. C.

Dalrymple, G. B., and M. O. Garcia (1980), Age and chemistry of volcanic rocks dredged from Jingū Seamount, Emperor Seamount chain, *Initial Rep. Deep Sea Drill. Proj*., vol. *55*, pp. 685–693, U.S. Gov. Print. Off., Washington, D. C.

Dilles, J. H., and P. B. Gans (1995), The chronology of Cenozoic volcanism and deformation in the Yerington area, western Basin and Range and Walker Lane, *Geol. Soc. Am. Bull.*, *107*(4), 474–486, doi:10.1130/0016–7606.

Doubrovine, P. V., B. Steinberger, and T. H. Torsvik (2012), Absolute plate motions in a reference frame defined by moving hot spots in the Pacific, Atlantic, and Indian oceans, *J. Geophys. Res.*, *117*, B09101, doi:10.1029/2011JB009072.

Duncan, R. A., and R. A. Keller (2004), Radiometric ages for basement rocks from the Emperor Seamounts, ODP Leg 197, *Geochem. Geophys. Geosyst.*, *5*, Q08L03, doi:10.1029/2004GC000704.

Frey, F. A., S. Huang, J. Blichert-Toft, M. Regelous, and M. Boyet (2005), Origin of depleted components in basalt related to the Hawaiian hotspot: Evidence from isotopic and incompatible element ratios, *Geochem. Geophys. Geosyst.*, *6*, Q02L07, doi:10.1029/2004GC000757.

Garcia, M. O., D. G. Grooms, and J. J. Naughton (1987), Petrology and geochronology of volcanic rocks from seamounts along and near the Hawaiian Ridge: Implications for propagation rate of the ridge, *Lithos*, *20*, 323–336.

Garcia, M. O., J. M. Smith, J. P. Tree, D. Weis, L. Harrison, and B. R. Jicha, (2013). Petrology, geochemistry and ages of lavas from Northwest Hawaiian Ridge volcanoes, in *The Origin, Evolution, and Environmental Impact of Oceanic Large Igneous Provinces*, edited by C.R. Neal, E. Erba, W. Sager, and T. Sano, Geological Society of America Special Paper, Geological Society of America, Boulder, CO, (in press).

Griffiths, R. W., and M. A. Richards (1989), The adjustment of mantle plumes to changes in plate motion, *Geophys. Res. Lett.*, *16*, 437–440.

Hawkins, J. W., P. F. Lonsdale, and R. Batiza (1987), Petrologic evolution of the Louisville seamount chain, in *Seamounts, Islands, and Atolls, Geophys. Monogr. Ser*., vol. *43*, edited by B. H. Keating et al., pp. 235–254, AGU, Washington, D. C.

Huang, S. C., and F. A. Frey (2005), Recycled oceanic crust in the Hawaiian Plume: Evidence from temporal geochemical variations within the Koolau Shield, *Contrib. Mineral. Petrol.*, *149*, 556–575.

Huang, S., M. Regelous, T. Thordarson, and F. A. Frey (2005), Petrogenesis of lavas from Detroit Seamount: Geochemical differences between Emperor Chain and Hawaiian volcanoes, *Geochem. Geophys. Geosyst.*, *6*, Q01L06, doi:10.1029/2004GC000756.

Iaffaldano, G., H.-P. Bunge, and T. H. Dixon (2006), Feedback between mountain belt growth and plate convergence, *Geology*, *34*, 893–896, doi:10.1130/G22661.1.

Iaffaldano, G., H. P. Bunge, and M. Bücker (2007), Mountain belt growth inferred from histories of past plate convergence: A new tectonic inverse problem, *Earth Planet. Sci. Lett.*, *260*, 516–523.

Ingersoll, R. V., and P. E. Rumelhart (1999), Three-stage evolution of the Los Angeles basin, southern California, *Geology*, *27*, 593–596, doi:10.1130/0091–7613.

Jackson, E. D., I. Koizumi, G. B. Dalrymple, D. A. Clague, R. J. Kirkpatrick, and H. G. Greene (1980), Introduction and summary of results from DSDP Leg 55, the Hawaiian-Emperor Hot-Spot Experiment, *Initial Rep. Deep Sea Drill. Proj*., vol. *55*, pp. 5–31, U.S. Gov. Print. Off., Washington, D. C.

Keller, R. A., M. R. Fisk, and R. A. Duncan (1995), Geochemistry and $^{40}Ar/^{39}Ar$ geochronology of basalts from ODP Leg 145, *Proc. Ocean Drill. Program Sci. Results*, *145*, 333–344.

Keller, R. A., M. R. Fisk, and W. M. White (2000), Isotopic evidence for Late Cretaceous plume-ridge interaction at the Hawaiian hotspot, *Nature*, *405*, 673–676.

Kerr, B. C., D. W. Scholl, and S. L. Klemperer (2005), Seismic stratigraphy of Detroit Seamount, Hawaiian-Emperor seamount chain: Post-hot-spot shield-building volcanism and

deposition of the Meiji drift, *Geochem. Geophys. Geosyst.*, *6*, Q07L10, doi:10.1029/2004GC000705.

Koppers, A. A. P. (2002), ArArCALC—Software for $^{40}Ar/^{39}Ar$ age calculations, *Comput. Geosci.*, *5*, 605–619.

Koppers, A. A. P., H. Staudigel, and J. R. Wijbrans (2000), Dating crystalline groundmass separates of altered Cretaceous seamount basalts by the $^{40}Ar/^{39}Ar$ incremental heating technique, *Chem. Geol.*, *166*, 139–158.

Koppers, A. A. P., J. Phipps Morgan, J. W. Morgan, and H. Staudigel (2001), Testing the fixed hotspot hypothesis using $^{40}Ar/^{39}Ar$ age progressions along seamount trails, *Earth Planet. Sci. Lett.*, *185*, 237–252.

Koppers, A. A. P., R. A. Duncan, and B. Steinberger (2004), Implications of a nonlinear $^{40}Ar/^{39}Ar$ age progression along the Louisville seamount trail for models of fixed and moving hot spots, *Geochem. Geophys. Geosyst.*, *5*, Q06L02, doi:10.1029/2003GC000671.

Koppers, A. A. P., M. D. Gowen, L. E. Colwell, J. S. Gee, P. F. Lonsdale, J. J. Mahoney, and R. A. Duncan (2011), New $^{40}Ar/^{39}Ar$ age progression for the Louisville hot spot trail and implications for inter–hot spot motion, *Geochem. Geophys. Geosyst.*, *12*, Q0AM02, doi:10.1029/2011GC003804.

Koppers, A. A. P., et al. (2012). Limited latitudinal mantle plume motion for the Louisville hotspot, *Nat. Geosci.*, *5*, 911–917, doi:10.1038/ngeo1638.

Kuiper, K. F., A. Deino, F. J. Hilgen, W. Krijgsma, P. R. Renne, and J. R. Wijbrans (2008), Synchronizing rock clocks of earth history, *Science*, *320*, 500–504.

Lanphere, M. A., and G. B. Dalrymple (2000), First-principles calibration of ^{38}Ar tracers: Implications for ages of $^{40}Ar/^{39}Ar$ fluence monitors, *U.S. Geol. Surv. Prof. Pap.*, *1621*, 10 pp.

Lonsdale, P. (1988), Geography and history of the Louisville hotspot chain in the Southwest Pacific, *J. Geophys. Res.*, *93*, 3078–3104.

Miller, M. S., B. L. N. Kennett, and V. G. Toy (2006), Spatial and temporal evolution of the subducting Pacific plate structure along the western Pacific margin, *J. Geophys. Res.*, *111*, B02401, doi:10.1029/2005JB003705.

Molnar, P., and J. Stock (1987), Relative motions of hot spots in the Pacific, Atlantic and Indian Ocean since late Cretaceous time, *Nature*, *327*, 587–591.

Molnar, P., and J. M. Stock (2009), Slowing of India's convergence with Eurasia since 20 Ma and its implications for Tibetan mantle dynamics, *Tectonics*, *28*, TC3001, doi:10.1029/2008TC002271.

Morgan, W. J. (1971), Convection plumes in the lower mantle, *Nature*, *230*, 42–43.

Müller, R. D., M. Sdrolias, C. Gaina, and W. R. Roest (2008), Age, spreading rates, and spreading asymmetry of the world's ocean crust, *Geochem. Geophys. Geosyst.*, *9*, Q04006, doi:10.1029/2007GC001743.

O'Connor, J. M., P. Stoffers, and J. R. Wijbrans (1998), Migration rate of volcanism along the Foundation Chain, SE Pacific, *Earth Planet. Sci. Lett.*, *164*, 41–59.

O'Connor, J. M., P. Stoffers, and J. R. Wijbrans (2001), En echelon volcanic Elongate Ridges connecting intraplate foundation chain volcanism to the Pacific-Antarctic spreading center, *Earth Planet. Sci. Lett.*, *189*, 93–102.

O'Connor, J. M., P. Stoffers and J. R. Wijbrans (2004), The foundation chain: Inferring hotspot-plate interaction from a weak seamount trail, in *Oceanic Hotspots*, pp. 349–372, edited by R. Hekinian, P. Stoffers, and J.-L. Cheminée, Springer-Verlag Berlin Heidelberg New York.

Pietruszka, A. J., and M. O. Garcia (1999), A rapid fluctuation in the mantle source and melting history of Kilauea Volcano inferred from the geochemistry of its historical summit lavas (1790–1982), *J. Petrol.*, *40*, 1321–1342.

Pringle, M. S., and G. B. Dalrymple (1993), *American Geophysical Union Geophysical Monograph*, *77*, edited by M. S. Pringle, W. W. Sager, W. V. Sliter, and S. Stein, American Geophysical Union, Washington D.C., pp. 263–277.

Raymond, C. A., J. M. Stock, and S. C. Cande (2000), Fast paleogene motion of the Pacific hotspots from revised global plate circuit constraints, in *The History and Dynamics of Global Plate Motions, AGU Geophysical Monograph*, edited by M. A. Richards, R. G. Gordon, and R. D. van der Hilst, AGU, Washington, D. C., doi:10.1029/GM121p0359.

Regelous, M., A. W. Hofmann, W. Abouchami, and S. J. G. Galer (2003), Geochemistry of lavas from the Emperor Seamounts, and the geochemical evolution of Hawaiian magmatism from 85 to 42 Ma, *J. Petrol.*, *44*, 113–140.

Renne, P. R., C. C. Swisher, D. B. Karner, T. L. Owens, and D. J. de Paulo (1998), Intercalibration of standards, absolute ages and uncertainties in $^{40}Ar/^{39}Ar$ dating, *Chem. Geol.*, *145*, 117–152.

Shafer, J. T., C. R. Neal, and M. Regelous (2005), Petrogenesis of Hawaiian postshield lavas: Evidence from Nintoku Seamount, Emperor Seamount Chain, *Geochem. Geophys. Geosyst.*, *6*, Q05L09, doi:10.1029/2004GC000875.

Sharp, W. D., and D. A. Clague (2006), 50-Ma initiation of Hawaiian-Emperor bend records major change in Pacific plate motion, *Science*, *313*, 1281–1284.

Sleep, N. H. (1996), Lateral flow of hot plume material ponded at sublithospheric depths, *J. Geophys. Res.*, *101*, 28,065–28,083.

Sleep, N. H. (2007), Origins of the plume hypothesis and some of its implications, in *Plates, Plumes, and Planetary Processes, Geol. Soc. Am. Spec. Paper*, edited by G. R. Foulger, and D. M. Jurdy, vol. *430*, pp. 29–45.

Small, C. (1995), Observations of ridge-hotspot interactions in the Southern Ocean, *J. Geophys Res.*, *100*, 17,931–17,946.

Smith, W. H. F., and D. T. Sandwel (1997), Global seafloor topography from satellite altimetry and ship depth soundings, *Science*, *277*, 1957–1962.

Steiger, R. H., and E. Jäger (1977), Subcommission on geochronology: Convention on the use of decay constants in geo- and cosmochronology, *Earth Planet. Sci. Lett.*, *36*, 359–362.

Steinberger, B. (2000), Plumes in a convecting mantle: models and observations for individual hotspots, *J. Geophys. Res.*, *105*, 11,127–11,152.

Steinberger B., and C. Gaina (2007), Plate-tectonic reconstructions predict part of the Hawaiian hotspot track to be preserved in the Bering Sea, *Geology*, *35*, 407–410, doi:10.1130/G23383A.1.

Steinberger, B., and R. J. O'Connell (2000), Effects of mantle flow on hotspot motion, in *The History and Dynamics of Global Plate Motions, Geophysical Monograph*, edited by M. A. Richards, R. G. Gordon, and R. D. van der Hilst, AGU, Washington, D. C., doi:10.1029/GM121p0377.

Steinberger, B., R. Sutherland, and R. J. O'Connell (2004), Prediction of Emperor-Hawaii seamount locations from a revised model of global plate motion and mantle flow, *Nature*, *430*, 167–173.

Tarduno, J. A., et al. (2003), The Emperor Seamounts: Southward motion of the Hawaiian hotspot plume in Earth's mantle, *Science*, *301*, 1064–1069.

Tarduno, J. A. (2007), On the motion of Hawaii and other mantle plumes, *Chem. Geol.*, *241*, 234–247.

Tarduno, J., H.-P. Bunge, N. Sleep, and U. Hansen (2009), The bent Hawaiian-Emperor hotspot track: Inheriting the mantle wind, *Science*, *324*, 50–53.

Vlastélic, I., and L. Dosso (2005), Initiation of a plume-ridge interaction in the South Pacific recorded by high-precision Pb isotopes along Hollister Ridge, *Geochem. Geophys. Geosyst.*, *6*, Q05011, doi:10.1029/2004GC000902.

Vlastélic, I., L. Dosso, H. Guillou, H. Bougault, L. Geli, J. Etoubleau, and J. L. Joron (1998), Geochemistry of the Hollister Ridge: Relation with the Louisville hotspot and the Pacific–Antarctic Ridge, *Earth Planet. Sci. Lett.*, *160*, 777–793.

Watts, A. B., J. K. Weissel, R. A. Duncan, and R. L. Larson (1988), Origin of the Louisville Ridge and its relationship to the Eltanin fracture zone system, *J. Geophys. Res.*, *93*, 3051–3077.

Wessel, P., and L. W. Kroenke (2007), Reconciling late Neogene Pacific absolute and relative plate motion changes, *Geochem. Geophys. Geosyst.*, *8*, Q08001, doi:10.1029/2007GC001636.

Wessel, P., and L. W. Kroenke (2008), Pacific absolute plate motion since 145 Ma: An assessment of the fixed hot spot hypothesis, *J. Geophys. Res.*, *113*, B06101, doi:10.1029/2007JB005499.

Wessel, P., and L. W. Kroenke (2009), Observations of geometry and ages constrain relative motion of Hawaii and Louisville plumes, *Earth Planet. Sci. Lett.*, *284*, 467–472.

Wessel, P., and W. H. F. Smith (1991), Free software helps map and display data. *Eos Trans. AGU*, *72*, 441–446.

Wessel, P., Y. Harada, and L. W. Kroenke (2006), Toward a self-consistent, high-resolution absolute plate motion model for the Pacific, *Geochem. Geophys. Geosyst.*, *7*, Q03L12, doi:10.1029/2005GC001000.

Whittaker, J. M., R. D. Müller, G. Leitchenkov, H. Stagg, M. Sdrolias, C. Gaina, and A. Goncharov (2007a), Major Australian-Antarctic plate reorganization at Hawaiian-Emperor bend time, *Science*, *318*, 83–86, doi:10.1126/science.1143769.

Whittaker, J. M., R. D. Müller, and M. Sdrolias (2007b), Revised history of Izanagi-Pacific ridge subduction, IBM07 NSF-Margins Workshop, Abstracts, p. 86, Honolulu, Hawaii.

Wilson, J. T. (1963), A possible origin of the Hawaiian Islands, *Can. J. Phys.*, *41*, 863–870.

Wolfe, C. J., S. C. Solomon, G. Laske, J. A. Collins, R. S. Detrick, J. A. Orcutt, D. Bercovici, and E. H. Hauri (2009), Mantle shear-wave velocity structure beneath the Hawaiian hot spot, *Science*, *326*, 1388–1390, doi:10.1126/science.1180165.

Yang, H.-J., F. A. Frey, and D. A. Clague (2003), Constraints on the source components of lavas forming the Hawaiian North Arch and Honolulu Volcanics, *J. Petrol.*, *44*, 603–627.